END

FILMED

	1.0	4.5	2.8	2.5
1.1		3.2	3.6	2.2
		4.0		2.0
				1.8
1.25	1.4	1.6		

MICROCOPY RESOLUTION TEST CHART
NATIONAL BUREAU OF STANDARDS-1963-A

UNCLASSIF

SECURITY CLASSIFICATIO

AD-A151 912

ATION PAGE

1a. REPORT SECURITY CLASSIFICATION	1b. RESTRICTIVE MARKINGS

2a. SECURITY CLASSIFICATION AUTHORITY	3. DISTRIBUTION/AVAILABILITY OF REPORT
Unclassified	Approved for Public Release;
2b. DECLASSIFICATION/DOWNGRADING SCHEDULE	Distribution is Unlimited

4. PERFORMING ORGANIZATION REPORT NUMBER(S)	5. MONITORING ORGANIZATION REPORT NUMBER(S)
	AFOSR·TR· 85-0259

6a. NAME OF PERFORMING ORGANIZATION	6b. OFFICE SYMBOL (If applicable)	7a. NAME OF MONITORING ORGANIZATION
Princeton University Dept. of Mech. & Aero. Engr.		AFOSR/NA

6c. ADDRESS (City, State and ZIP Code)	7b. ADDRESS (City, State and ZIP Code)
Engineering Quadrangle Princeton, N.J. 08544	Bolling AFB DC·20332

8a. NAME OF FUNDING/SPONSORING ORGANIZATION AIR FORCE OFFICE OF SCIENTIFIC RESEARCH	8b. OFFICE SYMBOL (If applicable) NA	9. PROCUREMENT INSTRUMENT IDENTIFICATION NUMBER AFOSR 81-0248

8c. ADDRESS (City, State and ZIP Code)	10. SOURCE OF FUNDING NOS.			
BOLLING AFB DC 20332-6600	PROGRAM ELEMENT NO.	PROJECT NO.	TASK NO.	WORK UNIT NO.
11. TITLE (Include Security Classification) High Temperature Catalytically Assisted Combustion	61102F	2308	A2	

12. PERSONAL AUTHOR(S)
F.V. Bracco, B.S.H. Royce, C. Bruno, D.A. Santavicca, Y. Stein

13a. TYPE OF REPORT	13b. TIME COVERED	14. DATE OF REPORT (Yr., Mo., Day)	15. PAGE COUNT
FINAL	FROM 01AUG81 TO 31JUL88	Undtd	68

16. SUPPLEMENTARY NOTATION

DTIC ELECTE MAR 29 1985

S D

17	COSATI CODES		18. SUBJECT TERMS (Continue on reverse if necessary and identify by block number)
FIELD	GROUP	SUB. GR.	Catalytic Combustion
			Perovskite Catalysts.

19. ABSTRACT (Continue on reverse if necessary and identify by block number)

Results of research on a two dimensional, transient catalytic combustion model and on a high temperature perovskite catalyst are presented. A recently developed two dimensional, transient model has been used to study the ignition of CO/air mixtures in a platinum coated catalytic honeycomb. Comparisons between calculated and measured steady state substrate temperature profiles and exhaust gas compositions show good agreement. A platinum doped perovskite catalyst has been proposed which will exhibit low temperature light off and high temperature stability. Preliminary tests using a perovskite powder with one percent by weight platinum are encouraging, showing very little change in surface activity when used with propane fuel. Variations in catalytic activity from sample to sample have also been found and after extensive testing the cause of these variations have not been identified. However, preliminary tests using Fourier transform infrared photoacoustic spectroscopy do indicate differences in the various catalyst samples that may be related to the difference in catalytic activity. The use of bench top oven and differential scanning calorimetry (OVER)

20. DISTRIBUTION/AVAILABILITY OF ABSTRACT	21. ABSTRACT SECURITY CLASSIFICATION
UNCLASSIFIED/UNLIMITED ☒ SAME AS RPT. ☐ DTIC USERS ☐	UNCLASSIFIED

22a. NAME OF RESPONSIBLE INDIVIDUAL	22b. TELEPHONE NUMBER (Include Area Code)	22c. OFFICE SYMBOL
JULIAN M TISHKOFF	(202) 767-4987	AFOSR/NA

85 03 12 113

DD FORM 1473, 83 APR EDITION OF 1 JAN 73 IS OBSOLETE. UNCLASSIFIED

SECURITY CLASSIFICATION OF THIS PAGE

DTIC FILE COPY

techniques for screening catalysts in terms of relative activity and aging characteristics has also been demonstrated.

Accession For

NTIS GRA&I	X
DTIC TAB	☐
Unannounced	☐
Justification	

By

Distribution/

Availability Codes

| Dist | Avail and/or Special |

TABLE OF CONTENTS

RESEARCH OBJECTIVES

The research objectives of the Princeton Catalytic Combustion Program for the period 8/81 to 7/83 have been both the formulation and testing of a transient, two-dimensional catalytic combustion model capable of predicting the light-off transient of catalytic combustors as well as the testing and evaluation of a platinum-doped perovskite catalyst in terms of its high temperature durability and low temperature light-off characteristics.

STATUS OF RESEARCH

The potential of catalytic combustion for application to stationary gas turbines [1-7], aircraft gas turbines [8-13], highway vehicle turbines [14-18], and boilers [6] has now been widely recognized. The utility of catalytic combustors rests upon their ability to operate efficiently over a much wider range of fuel air ratios than are imposed by the flammability limits of conventional gas burners. The catalytic combustor also has the advantages of low NO_x levels, uniform exit temperature profile, and combustion stability over broader ranges of equivalence ratio.

It could be argued convincingly that catalytic combustion is ready for extensive commercial use, however, areas in which further progress could be made can also be identified. Justifiable objectives for current research include lowering the ignition temperature and at the same time increasing durability at high temperature, reducing fatigue due to thermal stresses during transient operations, and developing design optimization tools to isolate promising ranges of the innumerable parameters (see Table 1). The first is a problem of physics of solids but the second and third are questions that can be addressed within the thermal sciences.

Two Dimensional, Transient Catalytic Combustion Model*

When honeycomb monoliths are used, as is often the case, the flow in the channels is generally laminar and convection and diffusion of mass, momentum and energy in the gas and thermal diffusion in the solid can be characterized quite

---

*This work has been submitted for publication to The Journal of Heat and Mass Transfer.

accurately. Elementary homogeneous and heoterogeneous reactions cannot, but global mechanisms of engineering usefulness can often be determined. The conservation equations for the gas and the solid represent all these processes and allow one to study their interactions as well. In their simplest, one dimensional form such equations have already been extensively and fruitfully used [19,20]. In particular, within the context of transient operations, notable is the work of T'ien [21] that revealed many of their essential features.

One-dimensional models have the considerable advantage of simplicity but are inherently limited in their resolution capabilities. They allow one to compute axial gradients through the use of global transfer functions for the controlling radial gradients. These functions can be very accurate for fully developed steady flows but require significant adjustments for transient entrance flows. For design optimization studies, two-dimensional models offer greater accuracy, since they allow one to resolve both axial and radial gradients, at greater computational costs. Through them one can compute also the thermal radial and axial gradients in the solid that are relevant to the problem of thermal fatigue. Our earlier two dimensional model [22-23] was only for the steady state of the gas within a channel of the monolith. It used measured wall temperatures instead of solving for the thermal gradients in the solid. Thus, it was mostly a tool for the detailed interpretation of measured quantities. In the work reported here the complete coupled two-dimensional transient equations for both solid and gas are solved, however, to limit computation costs, the reported solutions were obtained using the quasi-steady gas assumption already employed by T'ien in his one-dimensional model.

The reported work concerns the oxidation of mixtures of CO and moist air on platinum. The oxidation of CO is an important step in the combustion of hydrocarbons. Platinum was chosen because it is one of the best characterized cata-

---

4

lyst even though it is not the best one for catalytic combustion due to its limited high temperature durability. However, its low temperature ignition properties are excellent and it remains a good candidate for certain applications.

In the following sections, the time scales associated with the problem are considered first. Then the equations of the model are presented and a detailed discussion is given of one ignition transient. Finally steady state results computed through the transient are compared with measured ones (no transient measurements are available). Details can be found in [24].

Characteristic time scales

For a well-insulated, monolithic catalytic combustor with uniformly spaced channels, the study of the entire reactor can be reduced to the one of a single channel. Such a channel is shown in Fig. 1 and is considered here. The details of the specific catalyst considered are in Table 1. The characteristic time scales of this problem are listed in Table 2, following T'ien [21].

In computing the estimates of Table 2, averaged quantities were used. This precludes axial variations. Actually the time scales vary along the length of the channel. For example, in the entrance zone, the boundary layer growth is very fast and consequently the rates of transport vary rapidly, as well. Also, local sources and sinks of heat reduce local length scales. Thus the times of Table 2 are very rough estimates. Indeed, the substrate heat up time will ultimately be computed to be between 1 and 10 s instead of 60s. Nonetheless the estimates suggest some important simplications whose validity can always be checked aposteriori.

The characteristic times of the gas are shorter by about one order of magnitude than those of the solid so that the quasi-steady gas phase assumption may be justified in our case. However, the difference between gas and solid times is not overwhelmingly large and is sensitive to geometrical parameters.
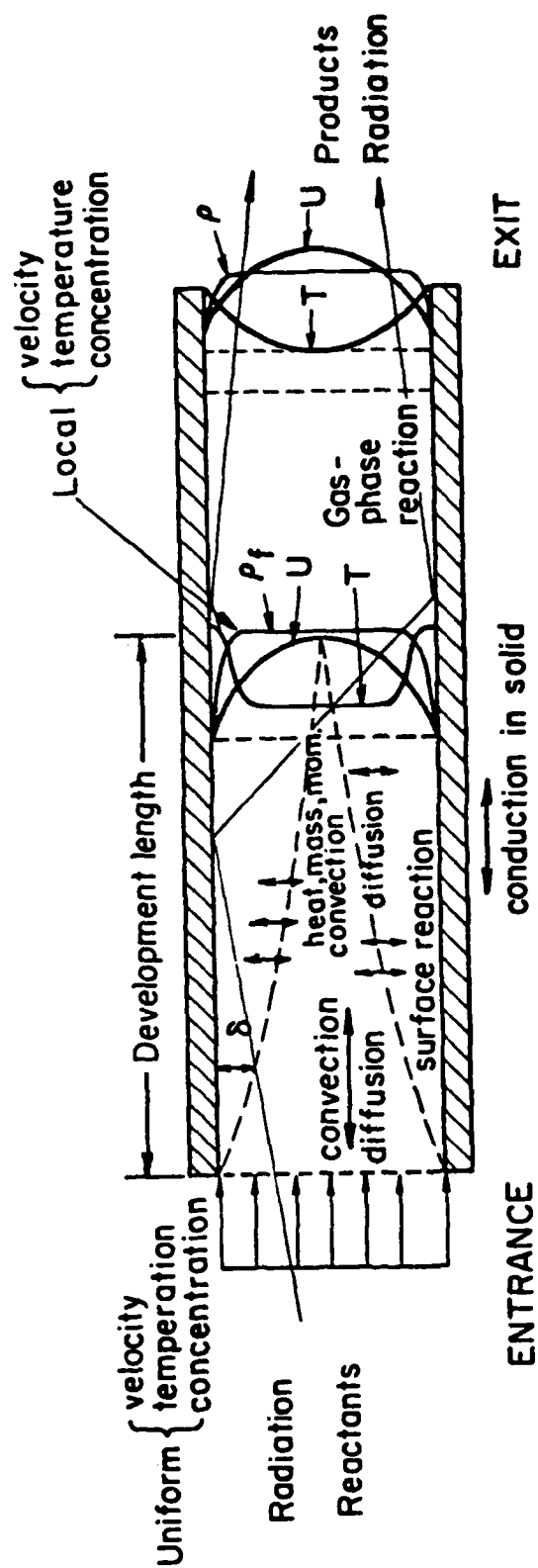
FIGURE 1. PHYSICAL AND CHEMICAL PROCESSES IN A CATALYST CHANNEL

TABLE 1. CATALYST PROPERTIES

SUBSTRATE: Cordierite, American Lava Corp., AlSiMag 795, split cell

length 0.0760 ± 0.003 m

wall thickness 0.25×10^{-3} m

open area 64%

channels per unit area 0.35×10^6 m^{-2}

open area per channel 1.9×10^{-6} m^2

ratio surface area to total volume 2100 m^2/m^3

ratio surface area to gas volume 3260 m^2/m^3

channel hydraulic diameter 0.0014 m

bulk density 610 kg/m^3

solid density 1700 kg/m^3

safe operating temperature 1473 K

specific heat 800 J/kg·K

coefficient of thermal expansion (linear, 294-1033 K) 3.8×10^{-6} K^{-1}

thermal conductivity of solid (572 K) 1.4 J/m·s·K

approximate channel cross-section is a trapezoid with base lengths .0011 m

   and .0023 m, and height .0012 m

WASHCOAT: γ-alumina

loading 115-125 kg/m^3

surface area (BET) $(29.2-33.0) \times 10^6$ m^2/m^3

CATALYST: platinum

loading 4.2 kg/m^3

surface area (CO chemisorption) 6×10^4 m^2/m^3

The γ-alumina and platinum were applied by Matthey Bishop, Inc., Malvern, PA.

TABLE 2

ESTIMATE OF TIME SCALES OF A CATALYTIC CHANNEL IN THE MONOLITH OF TABLE I

	TIME	DEFINITION	MAGNITUDE
1.	Gas residence time in reactor	L/U_{IN}	$(1.5 - 7.5) \times 10^{-3}$ s.
2.	Heat, mass & momentum transfer time between gas and catalyst surface	$\dfrac{1}{Nu_g}\dfrac{R^2}{\alpha_g}$	10^{-3} s.
3.	Homogeneous reaction time	$\left\{k_o \exp(-E_o/_{RT})[O_2][H_2O]^{1/2}\right\}^{-1}$	Variable depending on local fuel concentration and temperature
4.	Heterogeneous reaction time	$\left\{2\dfrac{k_s}{R}\exp(-E_{s/RT})\right\}^{-1}$	Variable depending on local fuel concentration and temperature
5.	Time for temperature wave to reach the substrate half thickness	$\dfrac{(s/2)^2}{\alpha_s}$	10^{-2} s.
6.	Time for temperature wave to reach the centerline of the gas channel	$\dfrac{R^2}{\alpha_g}$	3×10^{-3} s.
7.	Time for temperature wave to reach the end of the substrate	$\dfrac{L^2}{\alpha_s}$	5×10^3 s.
8.	Substrate heat-up time	$\dfrac{1}{Nu_g}\dfrac{\rho_s Cp_s}{k_g}A_s$	60 s.
9.	Input characteristic time		$10^{-3} - 10^{-1}$ s.

Thus the quasi-steady gas approximation cannot be assumed valid for all cataly-tic combustors of practical interest. Similarly, in the solid, the time for radial thermal equilibrium is much shorter than that for axial equilibrium and one would be justified in treating the solid as one dimensional, however the important thermal stresses would not be properly resolved. Our model does not require either one of the above two limitations, nonetheless, the reported results were obtained with the quasi-steady gas phase approximation to reduce computation costs. Radial gradients in the solid were, however, resolved.

Notice that associated with heterogeneous fuel conversion are two time scales: that for the surface reaction and that for the transfer of mass between the gas and the surface. When the former is much smaller than the latter fuel conversion is mass transfer limited. This is never the case at the beginning of the transient but is often the case in steady state.

Equations

The gas phase equations for the flow inside a channel schematized in Fig. 1, are the complete, two-dimensional, conservation equations for reactive, lami-nar flow [25]. For the experimental conditions investigated, the Reynolds number of the flow is below the critical one ($\sim$ 2000) for transition to tur-bulence.

The general conservation equation for the gas is written as

$$\frac{\partial \rho \phi}{\partial t} + \frac{1}{r} \left[\frac{\partial}{\partial x} (\rho r u \phi) + \frac{\partial}{\partial r} (\rho r v \phi) - \frac{\partial}{\partial x} \left(r \Gamma \frac{\partial \phi}{\partial x} \right) - \frac{\partial}{\partial r} \left(r \Gamma \frac{\partial \phi}{\partial r} \right) \right]$$

$$= S_\phi \qquad (1)$$

where ϕ $\qquad = u, v, T, y_k$, etc.

$\qquad \Gamma \qquad\qquad =$ appropriate transport property, such as μ, K, ρD_{ik}, etc.

$\qquad S_\phi \qquad\qquad =$ corresponding source term, such as $-\partial p / \partial x$ or the rate of species formation/destruction

$\partial \phi / \partial t$ = unsteady or inertial term

$\partial \rho / \partial x$ = axial

} convective terms

$\partial \rho / \partial r$ = radial

$\partial (r\Gamma \; \partial \phi / \partial x)/\partial x$ = axial

} diffusive terms

$\partial (r\Gamma \; \partial \phi / \partial r)/\partial r$ = radial

For the substrate only the energy conservation equation is necessary. It has the same form as the general conservation Eq. 1 except for exclusion of the convective and source terms:

$$\rho_w c_{p_w} \frac{\partial T}{\partial t} = \frac{1}{r} \left[\frac{\partial}{\partial x} \left(r \; K_w \frac{\partial T}{\partial x} \right) + \frac{\partial}{\partial r} \left(r \; K_w \frac{\partial T}{\partial r} \right) \right] \qquad (2)$$

All the model equations are given explicitly in Table 3. The laminar transient coefficients (μ, K, D_{ik}) and the specific heats varied from species to species and with temperature and were obtained from Refs. 26 and 27 respectively.

The approach utilized to solve the equations may be called a "continuum" approach. The solution algorithm makes no distinction between the gas phase and the substrate. The material properties change appropriately and the convective terms are set to zero for the substrate. Temperature matching at the interface is specified as a boundary condition. With this approach, the gas and the substrate energy equations are solved simultaneously and temperature matching at the interface is automatic.

Boundary and initial conditions

a) The boundary conditions used in the model are:

(i) At the inlet (x=0) of the gas phase, all physical variables are specified including the gas pressure and velocity. The fuel concentration increases with time until it reaches its final steady state value according to

$$Y_{CO}(\tau) = Y_{CO,F} \left[1 - \frac{\tau}{e^\tau - 1} \right]$$

(3)

and for $Y_{CO}(\tau) \geqslant 0.99 \, Y_{CO,F}$, $Y_{CO}(\tau) = Y_{CO,F}$

where τ = non-dimensional time = t/t^*

t = time

t^* = characteristic variable for fuel ramp

$\sim 10^{-3} - 10^{-1}$ sec.

$Y_{CO}(\tau)$ = fuel concentration at inlet

$Y_{CO,F}$ = fuel concentration at inlet at the end of the

fuel ramp.

(ii) At the outlet (x=L) of the gas phase, all physical variables ϕ have their gradients set to zero, i.e. $\partial \phi / \partial x = 0$. This linear condition simplifies the solution and is also observed in practice, provided the L/D ratio of the channel is (~ 100).

(iii) For the substrate, the only variable of interest is the temperature T. The axial temperature gradients must satisfy the radiative heat exchanges from the end faces of the catalyst to the upstream and downstream parts of the test section:

$$K_w \left(\frac{\partial T}{\partial x}\right)_{x=0} = \varepsilon\sigma \left(T_{f,o}^4 - T_{TS,IN}^4\right)$$

$$\text{(4)}$$

$$K_w \left(\frac{\partial T}{\partial x}\right)_{x=L} = \varepsilon\sigma \left(T_{f,L}^4 - T_{TS,OUT}^4\right)$$

where K_w = conductivity of the substrate

ε = emissivity of the substrate

σ = Stefan-Boltzmann constant

$T_{f,o}$, $T_{f,L}$ = temperature of the substrate face at $x = 0$ and $x = L$ respectively

$T_{TS,IN}$, $T_{TS,OUT}$ = temperature of the test-section at the inlet and the outlet respectively = 600 K

(iv) At the centerline of the channel $(r=0)$, the boundary conditions express radial symmetry, i.e. $\partial\phi/\partial r = 0$.

(v) At the half-thickness of the substrate $(r=R+s/2)$, small radial losses are present in the experiment in the magnitude of 10 K/channel [23]. To account approximately for them, the following temperature gradient is specified:

$$\left.\frac{dT}{dr}\right|_{r = R + \frac{s}{2}} = \frac{T_{NJWMI} - T_{NJW}}{\Delta r}$$

$$\text{(5)}$$

where T_{NJW} = temperature at the substrate half-thickness

T_{NJWMI} = temperature at the mesh point next to the substrate half-thickness

Δr = local radial cell length.

Assume $(T_{NJW} - T_{IN}) = C(T_{NJWMI} - T_{IN})$ then:

$$\frac{dT}{dr}\bigg|_{r = R + \frac{s}{2}} = (1-C)\frac{(T_{NJWMI} - T_{IN})}{\Delta r}$$

Thus, the simulation of radial losses is reduced to the specification of the single constant C. The value of C was 0.9985.

(vi) At the gas-substrate interface (r=R), the no-slip conditions for the gas apply, i.e. u = v = 0 and the temperature satisfies the balance between the catalytic heat release at the surface and conduction into the substrate and the gas phase

$$[(K_g \frac{\partial T}{\partial r})_R -] - [(K_s \frac{\partial T}{\partial r})_R +] = \dot{q}_{catalytic} \tag{6}$$

where K_g is the conductivity of the gas, K_s is the conductivity of the substrate, and $q_{catalytic}$ is the rate of heat release at the wall *per unit area.*

The chemical species, N_2 and H_2O are assumed inert and their radial gradients set equal to zero. When the reaction at the wall is not diffusion controlled, a kinetic rate is imposed for CO.

$$\rho\, D_{CO,N_2} \frac{\partial Y_{CO}}{\partial r}\bigg|_{r=R} = \dot{m}_{CO} \tag{7}$$

where $\dot{m}_{CO}$ is the CO mass consumption rate per unit area.

When the process gets diffusion limited, a switch to infinitely fast kinetics is made automatically and the boundary condition for CO becomes $Y_{CO} = 0$.

Further assuming that at the wall, CO is oxidized via the reaction $CO + 1/2\ O_2 \rightarrow CO_2$, the boundary conditions for O_2 and CO_2 are

$$\frac{\partial Y_{O_2}}{\partial r}\bigg|_{r=R} = \frac{1}{2}\frac{\partial Y_{CO}}{\partial r}\bigg|_{r=R} \cdot \frac{W_{O_2}}{W_{CO}} \cdot \frac{D_{CO,N_2}}{D_{O_2,N_2}}$$

(8)

$$\frac{\partial Y_{CO_2}}{\partial r}\bigg|_{r=R} = -\frac{\partial Y_{CO}}{\partial r}\bigg|_{r=R} \cdot \frac{W_{CO_2}}{W_{CO}} \cdot \frac{D_{CO,N_2}}{D_{CO_2,N_2}}$$

b) The initial conditions correspond to the situation when there is no fuel in the system. Non-reacting air at the initial temperature T_{IN} flows through the channel and the entire system is in equilibrium at this temperature. Therefore

$$T(x,r,0) = T_{IN}$$

$$Y_i(x,r,0) = 0 \qquad i = CO,\ CO_2 \qquad (9)$$

$$Y_i(x,r,0) = Y_{i,IN} \qquad i = O_2,\ N_2,\ H_2O.$$

Heterogeneous reaction

A vast literature [28-32] exists on the oxidation of CO on platinum. But the available rates apply to steady state. In the present study, one deals with a transient situation in which the fuel concentration at the surface of the catalyst changes rapidly. A qualitative study of the unsteady kinetics of the heterogeneous reaction of CO and oxygen on platinum was presented by Bykov and Yablonskii [33]. Conversion rates of the order of 10^{13} moles/cm^2-s were reported. The rates rise very rapidly with fuel concentration to these values

and then fall off sharply to the steady state values. There is a rate pulse which triggers the catalytic reaction. However, this was a low pressure study ($\sim 10^{-6}$ Torr) and there is uncertainty in extrapolating these results to our higher pressure ($\sim 10^{+3}$ Torr) situation.

In the absence of any concrete data, the reaction mechanism and rate expressions chosen are simple ones. The rate constant is kept sufficiently high to ensure that the rate of temperature rise of the system is compatible with that observed experimentally. The model chosen is a simple, one-step overall reaction corresponding to the reaction betwen adsorbed fuel and adsorbed oxygen:

$$CO + \frac{1}{2} O_2 \rightarrow CO_2$$
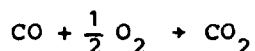
The reaction rate is taken as:

$$\frac{d[CO]}{dt} = - k_s \; [CO] \; \exp(-E_s/R^oT) \qquad \frac{moles}{cm^2-s} \qquad (10)$$
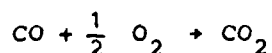
with $k_s = 3 \times 10^{17}$ cm/s, $E_s = 24.9$ kcal/mole, and [CO] is the concentration of CO near the wall in moles/cm^3.

The activation energy agrees with that used in [32,34,35] which cite overall rates.

Homogeneous kinetics

The model chosen for the homogeneous oxidation of CO by O_2 is a simple, one-step overall reaction:

$$CO + \frac{1}{2} O_2 \rightarrow CO_2$$

The reaction rate is taken as in [36,23]:

$$\frac{d[CO]}{dt} = -k_o [CO][O_2]^{0.5}[H_2O]^{0.5} \exp(-E_o/R^oT) \frac{moles}{cm^3-s} \qquad (11)$$

where $k_o = 1.3 \times 10^{14}$ cm^3/mole-s, $E_o = 126$ KJ/mole = 30 kcal/mole,
and [ ] = concentration in moles/cm^3

Radiation model

The test-section, which has a square cross section, is modeled as a cylinder. Radiation is thus simplified to the calculation of radiative losses from the front and back surfaces of the solid and the inside of a cylinder (the channel) to the inside of another cylinder (the modeled test-section). The angle factors for this geometry can be easily evaluated. The model computes the radiative loss from each computational element on the surface of the catalyst. Similarly, radiation inter-exchange between different elements on the catalyst surface is also evaluated [24]. In our case the net effect of radiation is heat losses that reduce the energy available for conduction from the interface into the gas and the solid.

Outline of the solution algorithm

All details of the solution technique are available in [24], including the listing of the program. Here only a brief outline is given.

The equations are solved numerically by a method based on the TEACH code documented by Gosman and Ideriah [37]. The code used in the present work differs from the original TEACH, that was for steady incompressible and nonreactive flows, by the introduction of species and energy conservation equations, variable density and the equation of state which links pressure, density and mass fractions and the extension to handle gas and solid simultaneously and through their transients.

The solution algorithm is as follows. The general Eq. 1 is integrated over the elemental cell volume, so that only convective and diffusive fluxes, and

sources appear inside the computer code. The partial differential equations for the conserved quantities are thereby transformed into linear finite difference equations which may be solved iteratively. The integration domain is divided into cells. For each variable a new line of values at each longitudinal location, x, is computed. Marching down the axis of the channel, the entire channel is swept. After the entire mesh has been swept, the total amount of conserved quantities is computed and compared with the entering fluxes. The process is repeated iteratively if the difference is above a set cut off, typically 5%.

A hybrid differencing scheme is used that reduces to upstream differencing for the convection terms if the absolute value of the cell Pellet number > 2 and to central differencing if < 2. The grid is finer near the entrance and the solid-gas interface and expands radially and axially from those two locations. Standard tests of increasing numerical resolution and of comparing numerical results with close form solutions for simpler cases were performed and are discussed in Ref. 24.

Complete transient solutions for the gas and the solid were obtained with an implicit time scheme, time steps of the order of 10^{-7} s, and about 100 iterations per time step. But the computation time was too long for parametric studies and the quasi-steady gas phase approximation was made. As explained in the introduction, this approximation is not always valid for practical combustors but is acceptable for the conditions of interest in this paper.

RESULTS

The general sequence of the computed transient events is as follows. Initially there is no CO in the channel. The CO concentration at the entrance of the channel is gradually increased to its final steady state value. (This fuel ramp occurs in a time which is short in comparison to that required for the entire system to reach its steady state configuration.) Thus at the beginning

the mixture is very lean and the temperature low. Conversion starts at the surface and its rate is controlled by the rate of the heterogeneous reaction. Due to the surface activity a boundary layer is formed that remains thin near the entrance but grows thicker along the length of the channel. Initially most of the heat is released near the entrance and goes to increase the temperature of both solid and the gas. The energy received by the gas near the entrance is convected downstream and diffused back to the solid, thus increasing its back temperature. Conduction along the solid occurs simultaneously. As the temperature of the system increases, homogeneous reactions start to contribute, surface reactions become faster than diffusion, and radiation losses become significant. The time to reach steady state is controlled by the heating of the back end of the solid. This sequence of events is in general agreement with that discussed by T'ien [21].

A detailed description of one transient is now given, followed by a comparison with measured substrate temperatures and exhaust emissions from a series of steady state experiments.

Transient study

This section contains the results for a case with the following final conditions at the inlet:

a)	Velocity	:	10 m/s
b)	Temperature	:	600 K
c)	Pressure	:	110 K Pa
d)	Equivalence ratio	:	0.32
e)	Adiabatic flame temperature	:	1580 K
f)	Water mole fraction	:	5.4×10^{-3}
g)	Mach number	:	0.02
h)	Reynolds number	:	290.4

It is one of the cases of Ref. 23 and its behaviour is typical for our system. Initially the temperature is 600 K everywhere and there is no fuel anywhere. The transient is begun by letting fuel into the system and the fuel time-ramp is shown in Fig. 2.

Overall results

The following energy balance can be written for the system:

$$
\begin{array}{ccc}
\text{rate of} & \text{rate of} & \text{rate of} \\
(\text{chemical energy})_{in} + & (\text{kinetic energy})_{in} + & (\text{thermal energy})_{in}
\end{array}
$$

$$
= (\text{rate of chemical energy})_{out} + (\text{rate of kinetic energy})_{out}
$$

$$
+ (\text{rate of thermal energy})_{out} + (\text{rate of radiation loss from}
$$

within the channel) + (rate of thermal energy into the substrate)

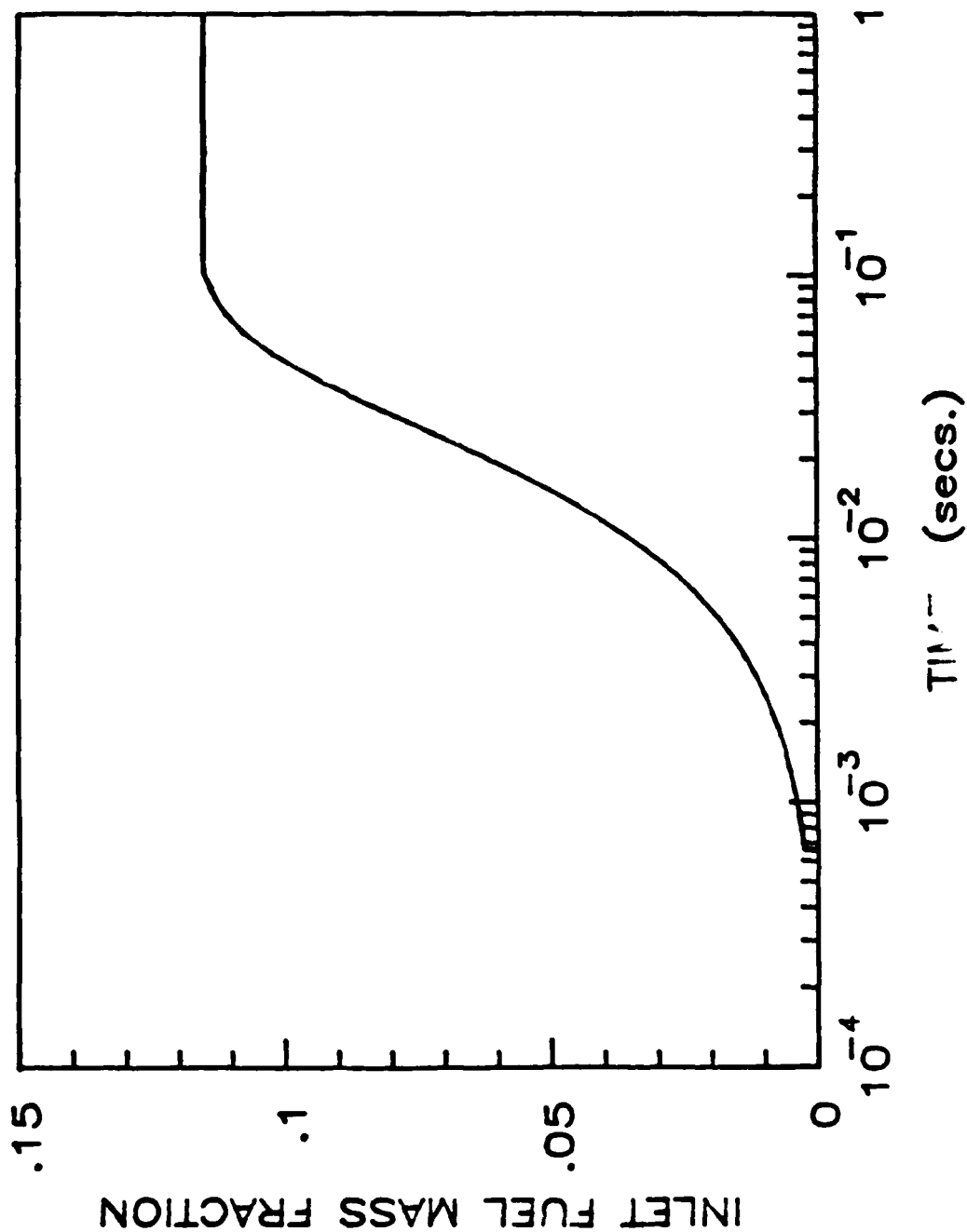The following definitions are introduced ($\eta_1 + \eta_2 + \eta_3 + \eta_4 + \eta_5 = 1$):

FIGURE 2.   VARIATION OF FUEL CONCENTRATION AT THE INLET DURING
             THE TRANSIENT

$$\eta_1 = \frac{\text{(rate of thermal energy)}_{out} - \text{(rate of thermal energy)}_{in}}{\text{(rate of chemical and kinetic energy)}_{in}}$$

$$\eta_2 = \frac{\text{(rate of radiation loss from the channel)}}{\text{(rate of chemical and kinetic energy)}_{in}}$$

$$\eta_3 = \frac{\text{(rate of thermal energy into the substrate)}}{\text{(rate of chemical and kinetic energy)}_{in}} \qquad (12)$$

$$\eta_4 = \frac{\text{(rate of kinetic energy)}_{out}}{\text{(rate of chemical and kinetic energy)}_{in}}$$

$$\eta_5 = \frac{\text{(rate of chemical energy)}_{out}}{\text{(rate of chemical and kinetic energy)}_{in}}$$

Fig. 3 shows the energy distribution during the transient and represents an overall picture of the transient processes. Notice first that the imposed fuel transient at the inlet lasts less than 0.1 s and the system reaches steady state at about 10s. Thus, the results do reflect the transient characteristics of the catalyst and not those of the fuel delivery system.

Initially, all the energy release goes into heating the substrate. As shown by the behaviour of η_3. This is true until $t \sim 0.1$s when the final fuel concentration gets established at the inlet. The initial heat release occurs on the surface of the catalyst. The process of equilibrating all the substrate but its entrance begins towards the end of the fuel ramp. This can also be seen by the stabilization of the radiation losses η_2 at a value fairly close to the final one (Radiation losses occur primarily from the front of the catalyst). At the same time the energy content of the gas phase, η_1, is increasing. This has
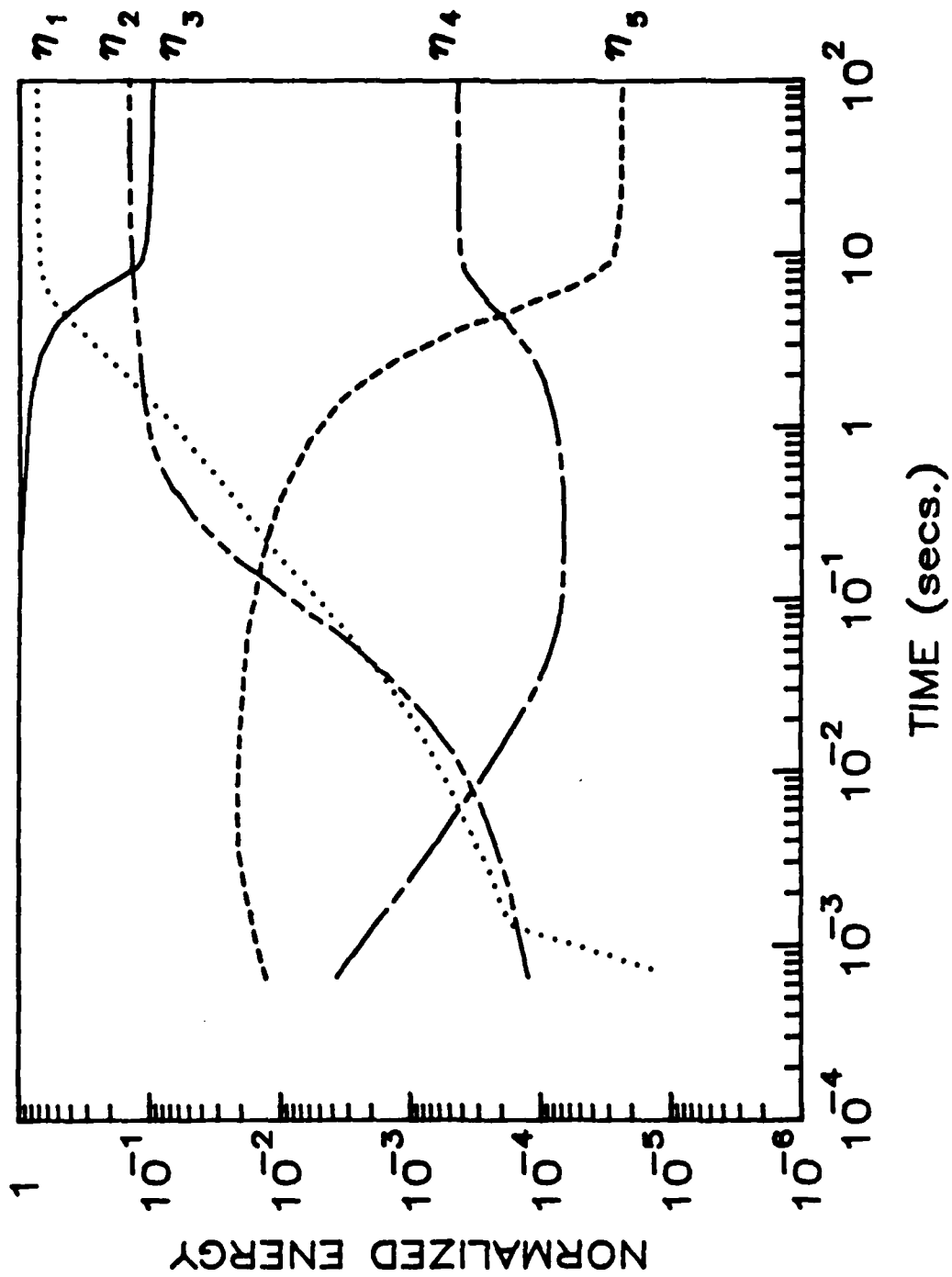
FIGURE 3.   DISTRIBUTION OF INCOMING ENERGY DURING THE TRANSIENT

two effects. Homogeneous reactions start playing a more important role and very little unburnt fuel finds its way to the exhaust. This is shown by the drop in η_5. The increase in the thermal content of the gases also manifests itself in the form of higher kinetic energy and is shown by the increase in η_4.

The term η_3 is significant in that it gives the transient time of the system. At steady state, the net energy flowing into the substrate is equal to that radiated by the front and back surfaces of the channel and lost radilly to adjacent channels. In this case, it amounts to about 20% of the chemical and kinetic energy flowing in.

Fig. (4) compares the overall conversion by the heterogeneous and homogeneous paths. The quantity being plotted is:

$$r_{GS} = \frac{\int_V \dot{\omega}_g \, dV}{\int_A \dot{\omega}_s \, dA} \tag{13}$$

The numerator is the overall rate of destruction of CO due to homogeneous reactions, while the denominator expresses the corresponding catalytic conversion rate. As indicated by the earlier plots, during the early part of the transient, fuel conversion is entirely due to the catalyst. This is an expected result since the light-off temperature for the catalytic reaction is low. This situation remains unchanged till almost steady state when the gas temperature is high enough for the gas phase reactions to start playing a more dominant role. This ratio reaches a steady value of about 10% at $t \sim$ 10s. Heterogeneous chemical kinetics is, thus, indispensable to ignition, feeding back into gas phase the heat necessary to raise its temperature and make secondary gas phase oxidation possible.
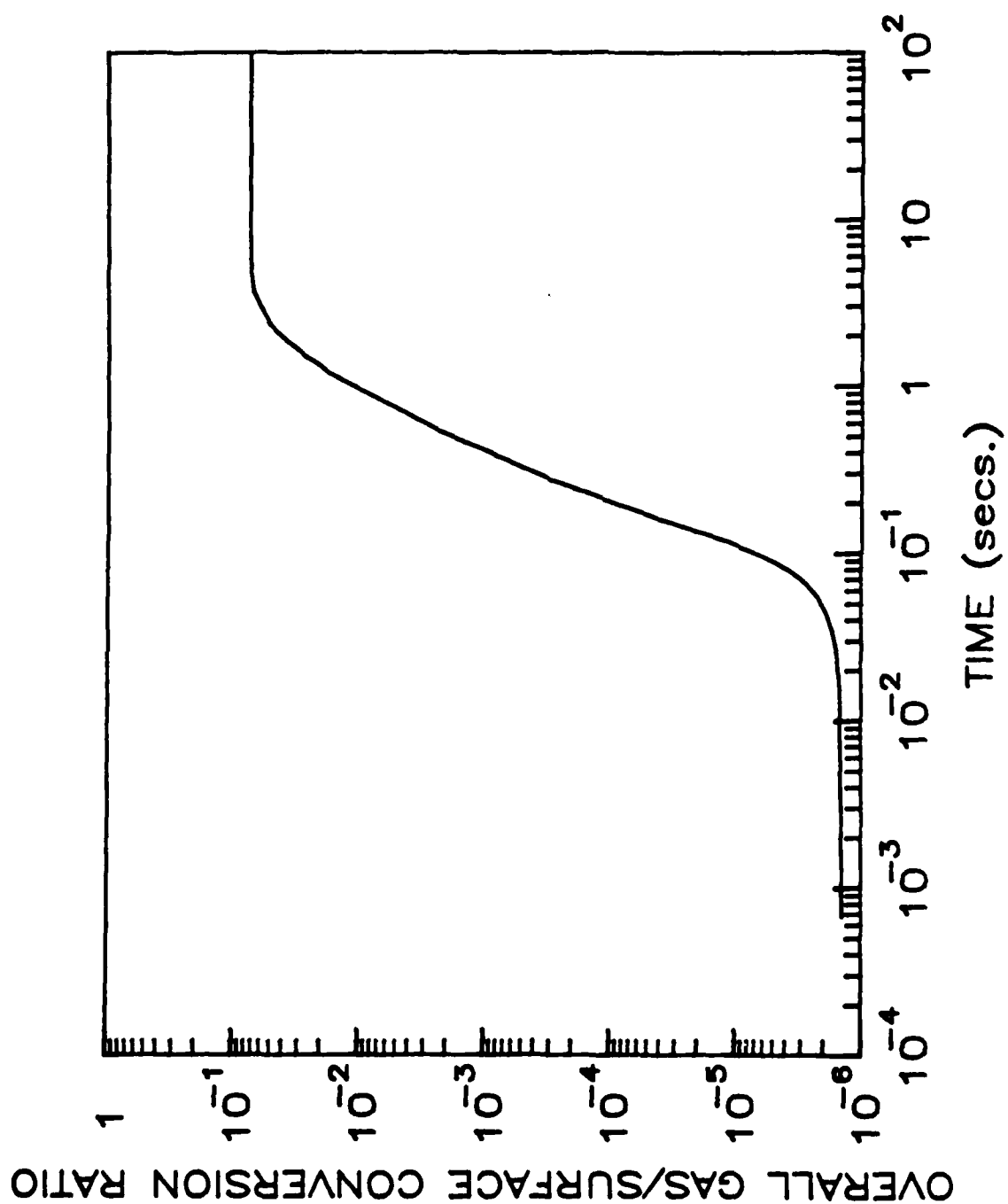
FIGURE 4. OVERALL GAS PHASE TO SURFACF CONVERSION
RATIO DURING THE TRANSIENT

Detailed results

Fig. (5) shows the axial variation of the ratio of fuel conversion by cata-
lytic reaction to that by gas phase oxidation. The quantity being plotted is:

$$r_{gs}(x) \equiv \frac{\sigma \int \dot{\omega}_g \, d\sigma \, \Delta x}{\ell \int \dot{\omega}_s \, d\ell \, \Delta x} \tag{14}$$

where σ : area of the channel

ℓ : perimeter of the channel

Δx : the local cell length.

The numerator is the net homogeneous conversion rate at an axial location
while the denominator is the local heterogeneous conversion rate. Initially,
the mixture is very lean and conversion of fuel is restricted to the surface of
the catalyst. This trend changes as the incoming fuel mixture turns richer and
the catalyst heats up. The contribution of homogeneous kinetics increases more
rapidly near the inlet of the channel where the temperature of the catalyst
rises more rapidly and heat is transferred to the gas. As the temperature of
the rear end comes up, gas phase contributions increase there, too. Finally, at
steady state, homogeneous and heterogeneous kinetics become comparable near the
midpoint of the channel. However, very little conversion takes place in abso-
lute terms at this location. Most of the fuel is used up near the inlet, and
where the homogenerous reactions still play a minor role.

Figs. (6a), (6b) and (7) provide a description of the axial redistribution
of thermal energy during the transient. For it, the following quantities are
defined:

$$\dot{q}_{catalytic} = \dot{q}_s + \dot{q}_G + \dot{q}_R + \dot{q}_L \tag{15}$$
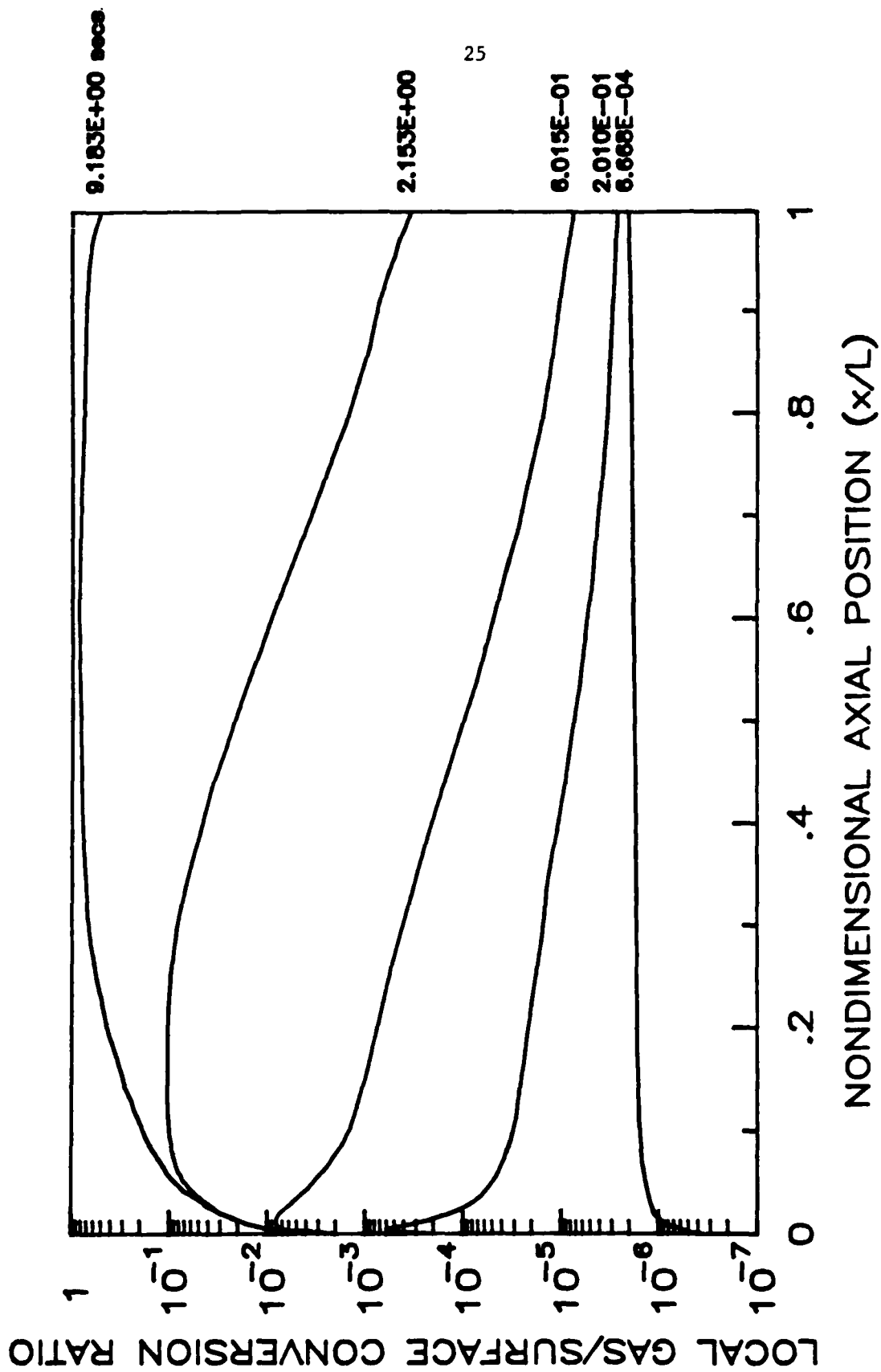
FIGURE 5.   AXIAL PROFILES OF GAS PHASE TO SURFACE
CONVERSION RATIO

where $q_{catalytic}$:   local rate of catalytic heat release

        $\dot{q}_s$:   local rate of heat storage in the substrate

        $\dot{q}_G$:   local rate of heat diffusion into the gas phase

        $\dot{q}_R$:   local rate of radiant heat loss

        $\dot{q}_L$:   local rate of conductive radial heat loss from the substrate

or $Q_S + Q_G + Q_R + Q_L = 1$, upon normalizing by $\dot{q}catalytic$.   (16)

In Fig. (6a), Q_S is shown at different times. Initially, the profile is a straight line with $Q_S \sim 1$. This implies that all the heat released goes into the substrate. With time, the axial profiles readjust. While near the entrance, the profile comes down to $Q_S \sim 0$, toward the exit, it rises so that $Q_S \gg 1$. This indicates that the front end of the catalyst has equilibrated while the rear gets heated by the hotter gas (the gas gets heated by the solid near the entrance). As time advances, the entire axial profile is seen to gradually return toward the dotted line, representing the steady state.

In Fig. (6b), Q_G, the normalized heat flux into the gas is shown and is seen to be almost a mirror image of Fig. (6a). Initially, heat transfer into the gas is negligible and $Q_G \sim 0$. A period of readjustment corresponding to that for the substrate begins. During this period, $Q_G \sim 1$ near the inlet which indicates that most of the energy released goes towards heating the gas. Toward the exit, Q_G is a large negative number. This is a direct evidence that the gas heated by the solid near the entrance, travels downstream and then heats the solid. Finally, the profile converges toward the dotted line, representing the steady state.
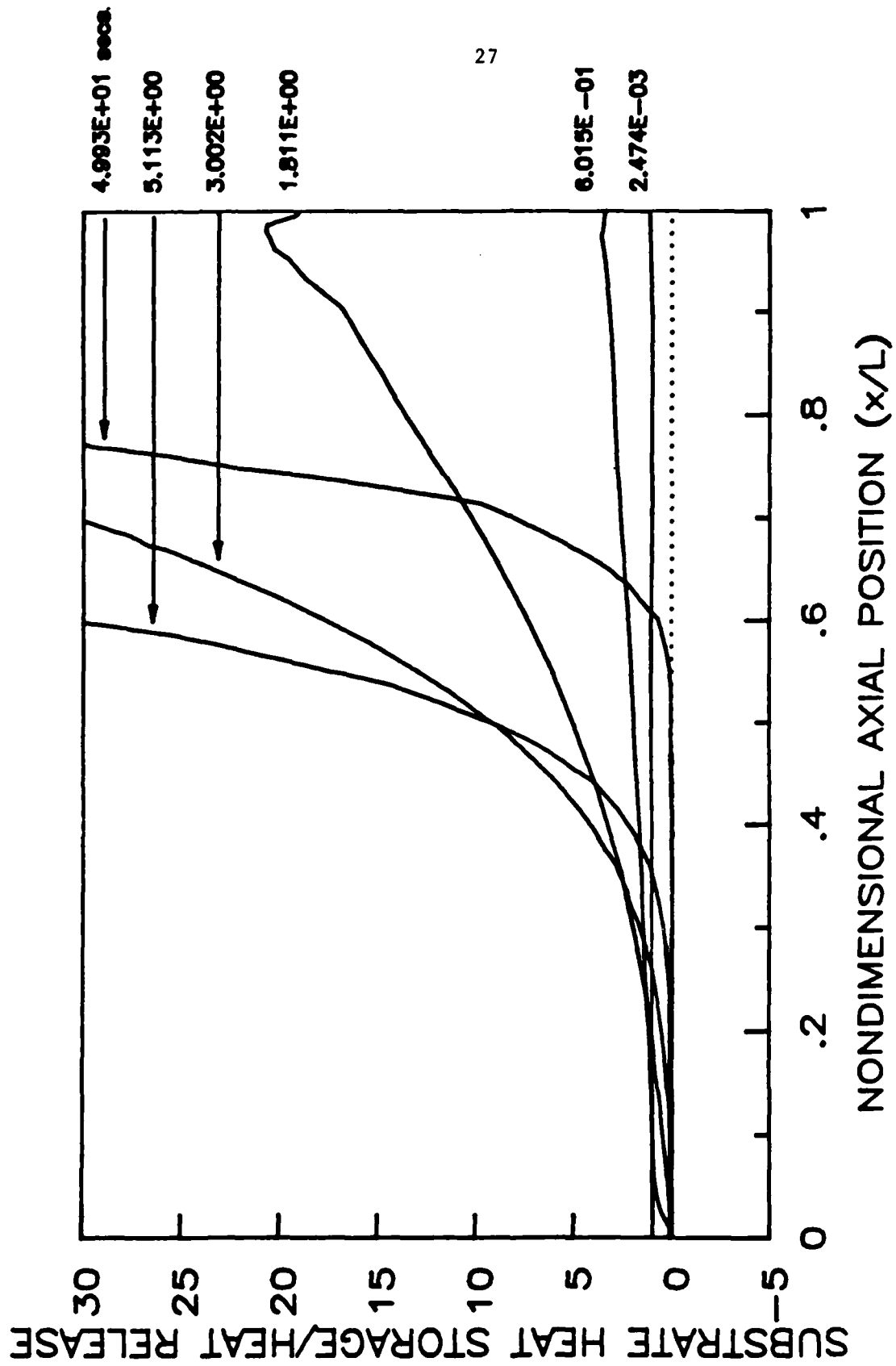
FIGURE 6a.   AXIAL PROFILES OF HEAT FLUX FORM THE INTERFACE TO THE SUBSTRATE
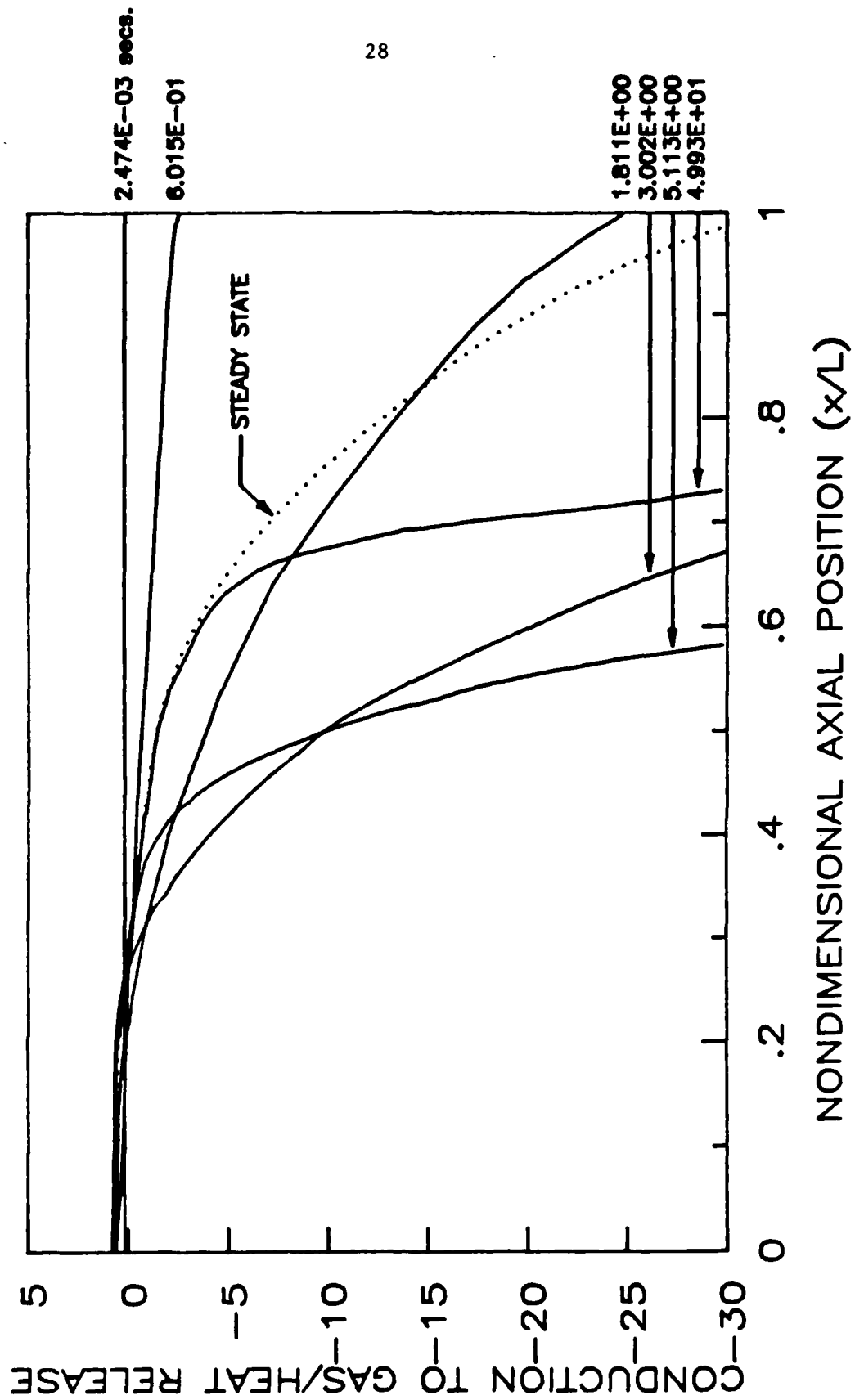
FIGURE 6b.   AXIAL PROFILES OF HEAT FLUX FROM THE INTERFACE TO THF GAS

Radiative losses rise rapidly with time but decrease sharply with the distance from the inlet, as seen in Fig. (7). Due to the large L/D ratio of the channel, radiation ceases to be of significance after 2 or 3 diameters into the channel, and only the first 10% of the channel is shown. A similar situation is present at the rear end of the catalyst. However the associated time scale is different since the rear end of the catalyst takes a long time heating up. Also, due to the rear end of the test section getting heated by the exhaust gases, the fractional radiation exchange is significantly lower in comparison to that at the inlet.

Fig. (8) shows axial temperature profiles at different radial locations, from the gas centerline to the substrate half-thickness, and Fig. 9 shows radial temperature profiles at different axial locations. Two time scales can be identified. The shorter one is the time required by the first tenth of the substrate to reach its steady state. The time required is about 0.1s which is of the same order as the period of the fuel ramp. It suggests that near the entrance the temperature will equilibrate as fast as the fuel is supplied. The other time scale is the substrate equilibration time and, as seen earlier, it is about 10s. The characteristic time for axial heat diffusion in the substrate (Table 2) is of the order of 10^3s. The significant reduction in the substrate heat up time is due to the heating of the back part of the solid by the gas and to the presence of axial heat sources.

Comparison with steady state measurements

No transient data are available for comparison with our computations. However the steady state computed through the transient can be compared with available steady state data [23]. It is realized that for the validity of the transient model satisfactory agreement with steady state data is necessary but not sufficient.
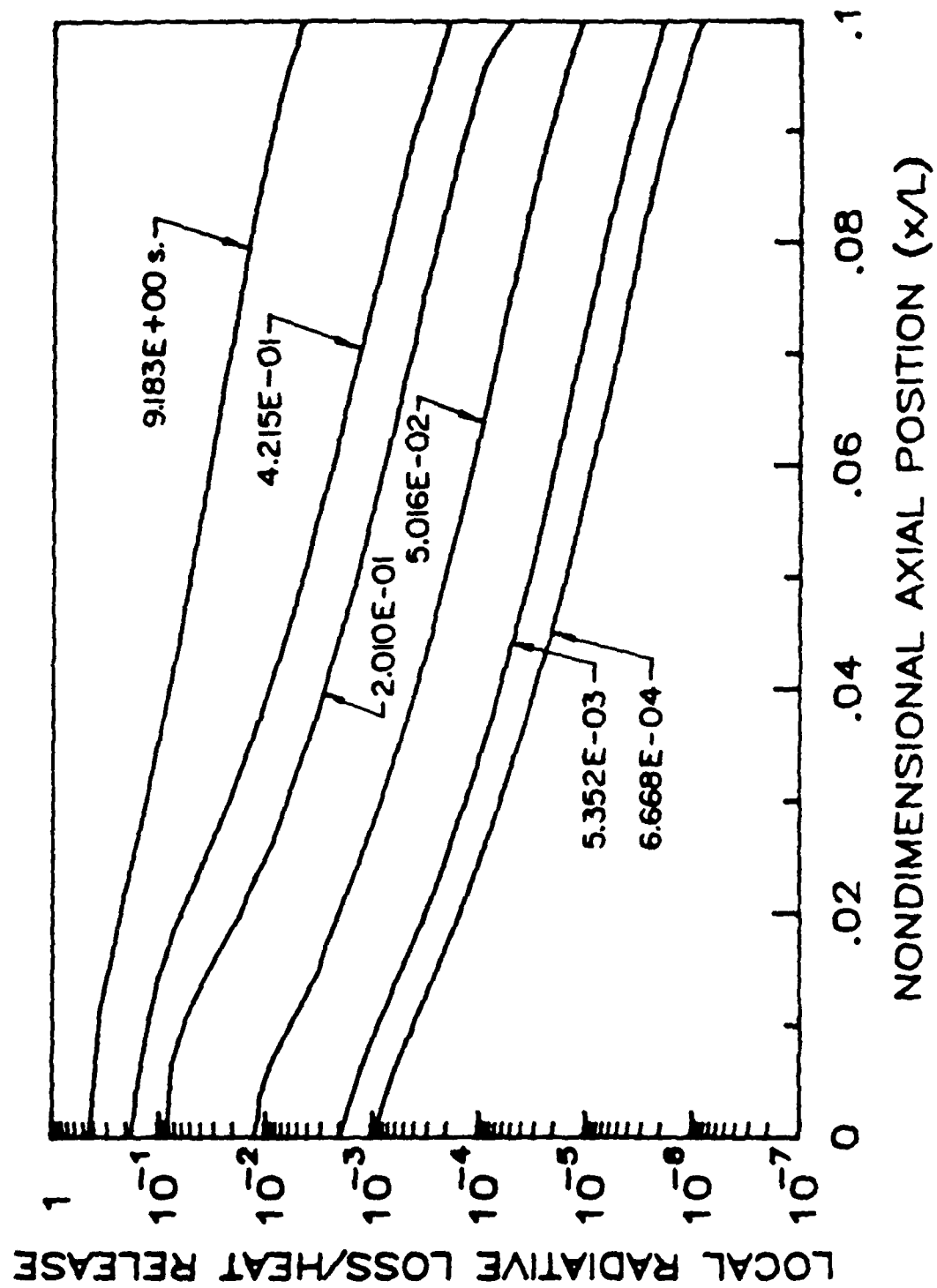
FIGURE 7.   AXIAL PROFILES OF RADIANT FLUX FROM THE INTERFACE
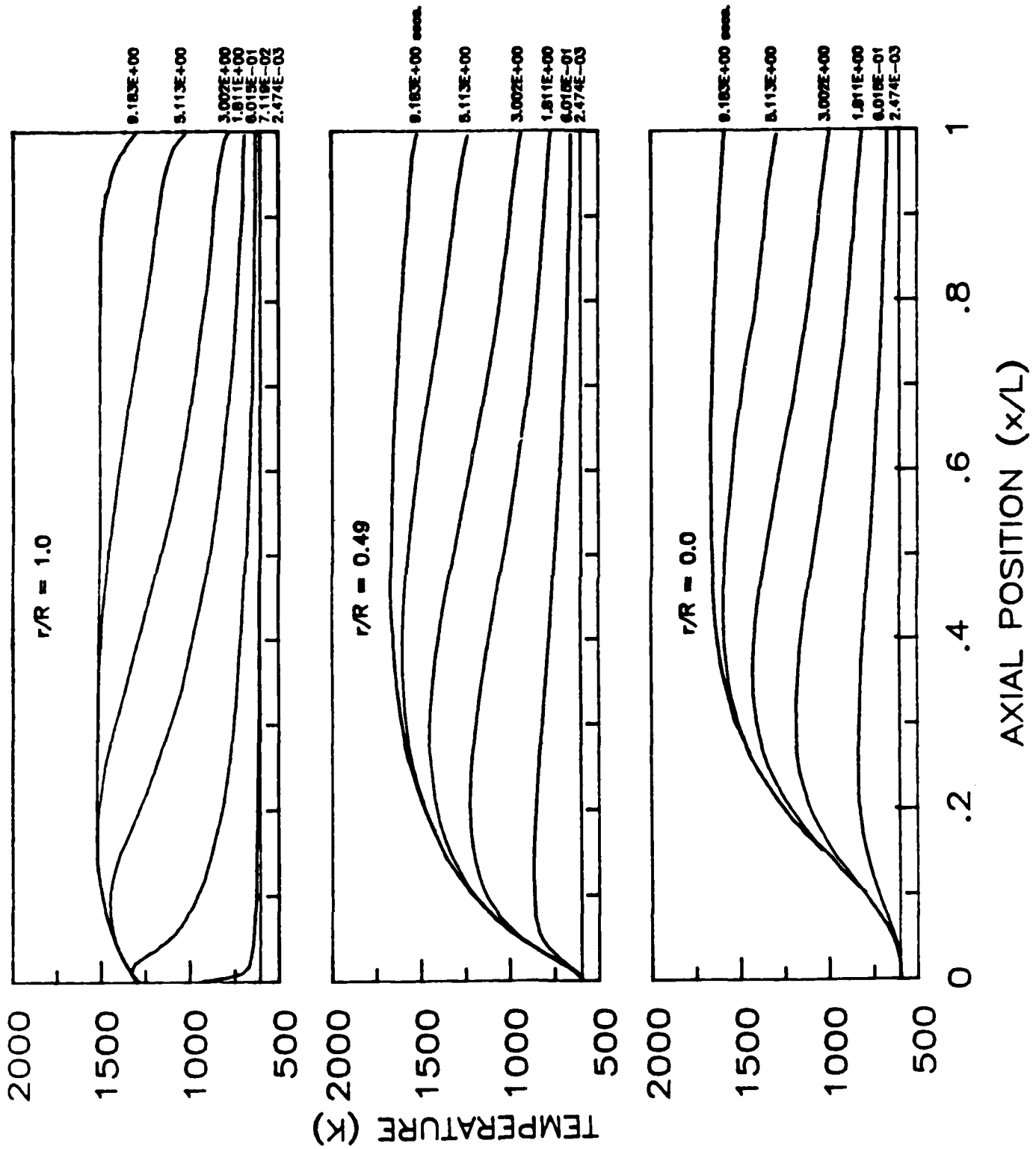
31

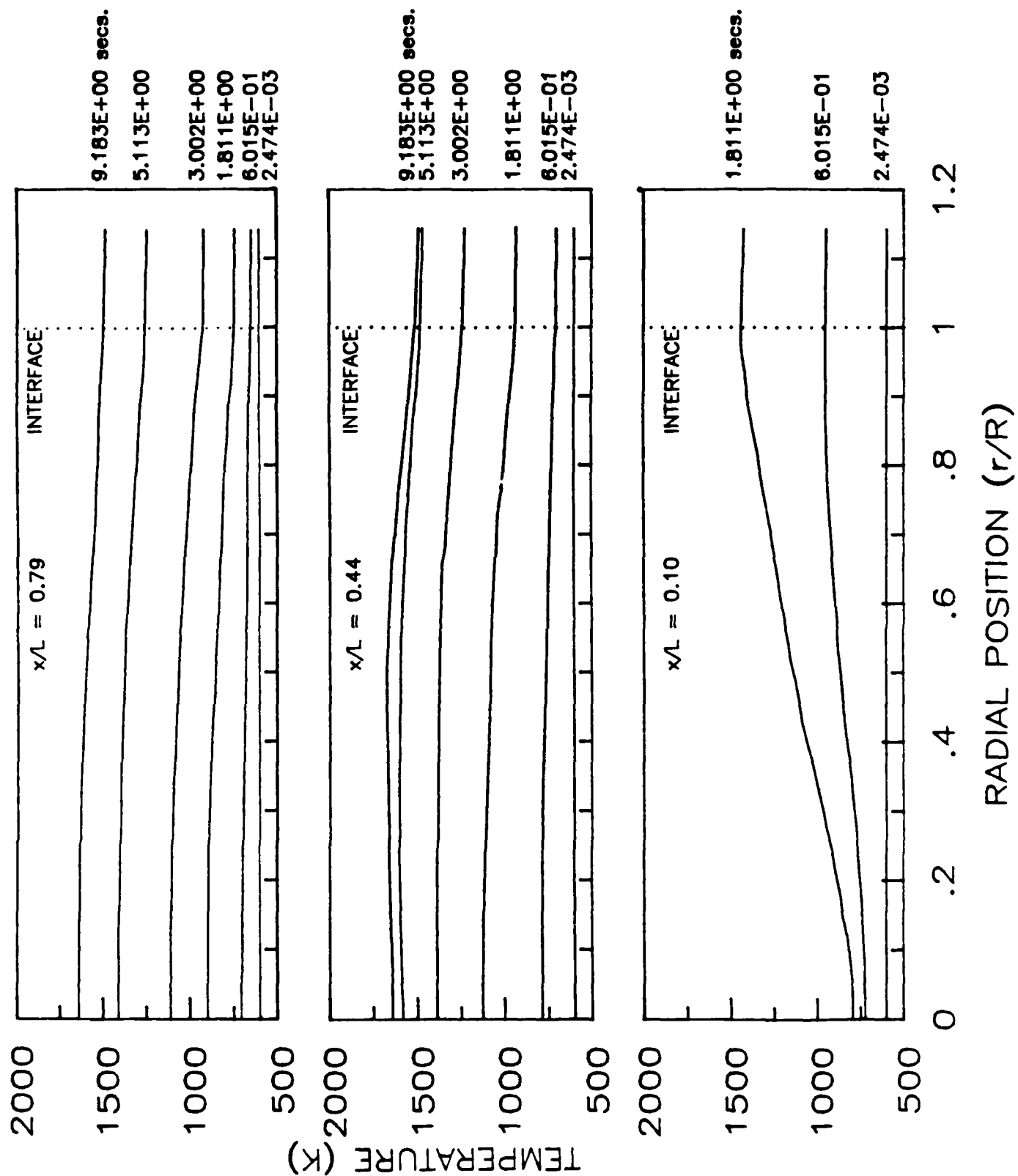FIGURE 8.   AXIAL TEMPERATURE PROFILES

FIGURE 9.   RADIAL TEMPERATURE PROFILES

Comparisons were made with cases differing in equivalence ratio and mixtures velocity, keeping the inlet temperature constant. Computed and measured wall temperatures compare favorably as shown in Fig. (10), and so do predicted and measured exhaust emissions (Fig. 11). A detailed discussion of the steady state can be found in Ref. 23. Overall the results indicate the predominance of diffusion rather than kinetics.

CONCLUSIONS

Following are the main conclusions.

The initial heat release occurs near the entrance at the interface, is controlled by heterogeneous reactions, and goes to heat the solid locally.

The temperature of the solid near the entrance achieves almost its final value before significant heating of the rest of the solid starts. The final temperature of the solid near the entrance is strongly influenced by radiation losses. Large spatial and temporal temperature gradients occur in the solid near the entrance controlled mostly by the availability of fuel. These gradients may be significant as far as fatigue due to thermal stresses is concerned.

The gas is heated first in the boundary layer near the entrance where significant radial and axial gradients are present.

The gas heated near the entrance flows downstream and heats the back of the solid. This process and surface reactions, rather than conduction along the solid, are the main mechanisms through which the back is heated.

Homogeneous reactions start being significant first in the boundary layer near the entrance, but for the conditions of our study their contribution to the overall oxidation of CO is small in comparison to that of heterogeneous reactions.

Heterogeneous oxidation of CO soon becomes diffusion controlled even though the entire light off transient is initially controlled by heterogeneous reaction
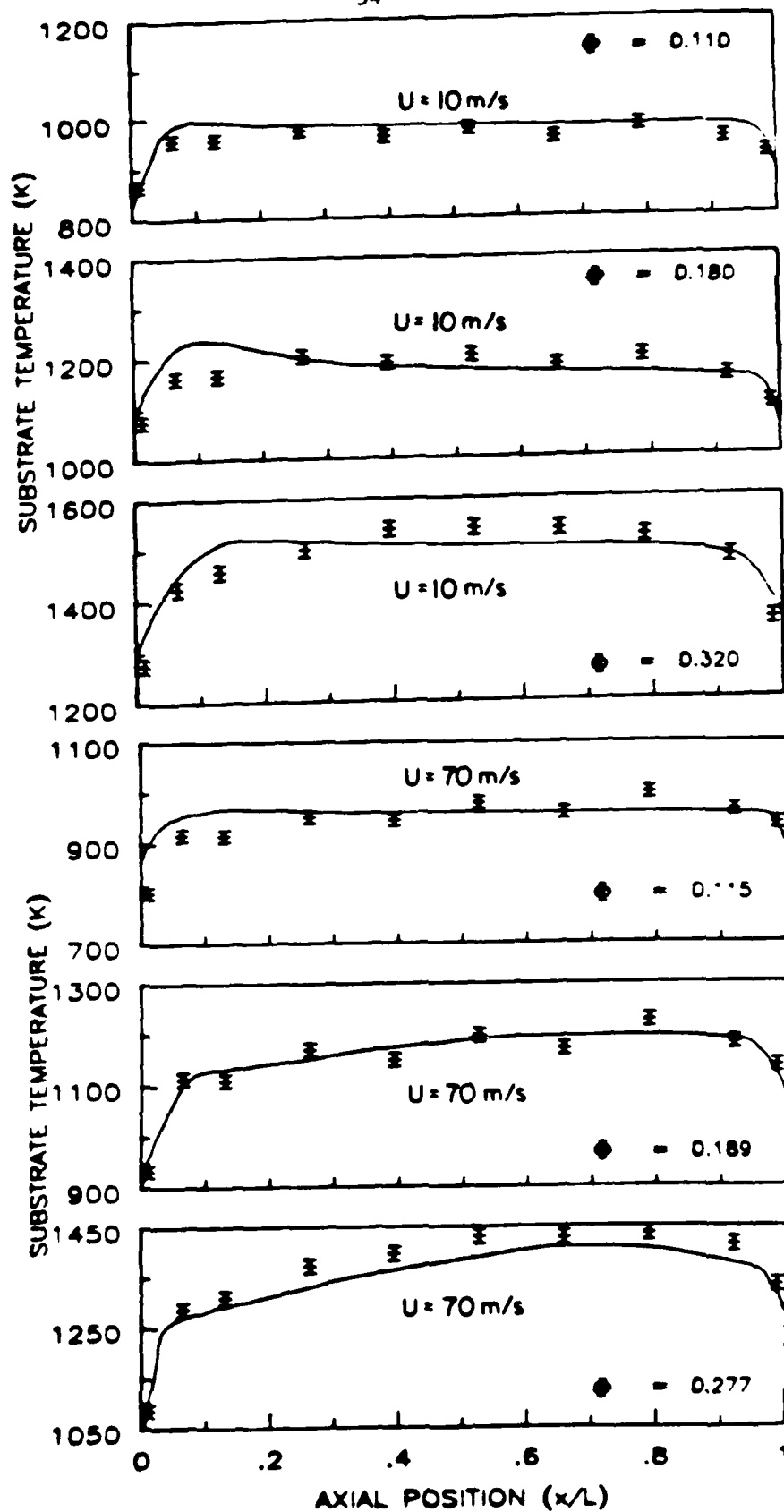
34

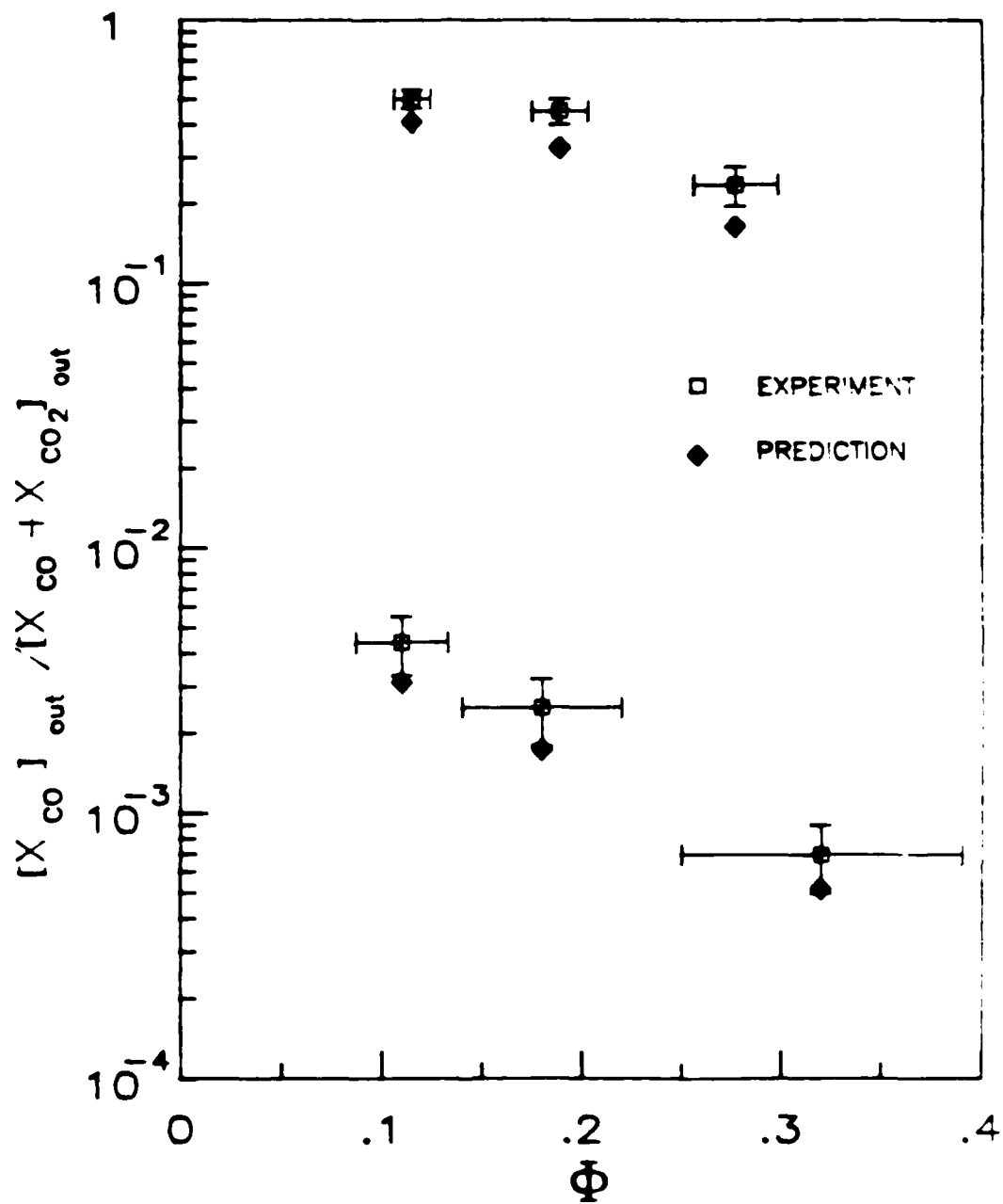FIGURE 10.   COMPARISON OF STEADY STATE TEMPERATURE PROFILES

FIGURE 11.   COMPARISON OF EXHAUST EMISSION

rates.

The overall equilibration process is governed by the thermal inertia of the substrate and by forced convection. 99% of steady state is achieved in about 10 s at a gas velocity of 10 m/s and in 1.5 s at 70 m/s for the particular substrate substance and geometry that was studied. The quasi-steady gas phase approximation was acceptable for our cases but only marginally so and should not be assumed to be valid for most honeycomb monoliths of practical interest.

Radiation significantly modifies both transient and steady state, particularly near the entrance but also near the exit, even though the energy involved is small and because of its localized concentration.

Perovskite Catalysts for High Temperature Catalytic Combustion*

The realization of catalytic combustion in practical combustion systems has in part been limited by the inadequacies of currently available combustion catalysts. One of the objectives of Princeton's Catalytic Combustion Program has been the development of combustion catalysts with improved high temperature (> 1500°K) stability in terms of erosion, corrosion, and thermal stress characteristics and improved performance characteristics in terms of lower ignition temperatures, extended flammability and blowout limits, and wider fuel tolerances.

In this section results are presented of a study of the high temperature durability and low temperature ignition characteristics of platinum doped perovskite catalysts. Operating temperatures of catalytic combustors often exceed 1500°K, resulting in unacceptably short lifetimes for standard catalysts. A good example of this is the case of platinum catalysts which have very good low temperature light off characteristics, however when such catalysts are operated at typical combustor temperatures, e.g. 1500°K, the platinum coating is lost through vaporization. The combustor will continue to operate normally since at these elevated temperatures the ceramic substrate will be sufficiently catalytic so as to make the combustor's performance diffusion controlled; however, when the combustor is shut off, reignition at the same operating conditions will not be possible since the onset of ignition is controlled by the low temperature surface reactions.

A new catalyst has been designed to exhibit long lifetime at high temperatures and adequate ignition characteristics at low temperatures. The catalyst is a modified perovskite based on $La(Cr_{0.5}Al_{0.5})O_3$. This ceramic has been

---

* Part of this work was presented at the Eastern States Section of the Combustion Institute Fall Meeting, December 1982.

doped to make it electrically conductive, and consequently it can be resistively heated to bring the catalyst up to the required light-off temperature. In addition, platinum has been incorporated into the crystal structure to give improved low temperature light-off while having a low platinum vapor pressure at high operating temperatures.

This catalyst can be used in powdered form, by washcoating it onto a high temperature ceramic substrate, or as sintered monolithic structures, e.g. plates. The advantage of using the catalyst in the form of plates is that they can be resistively heated to assist light-off. However, the catalyst is more readily available in powdered form and therefore the first tests with the new catalyst have been made with it washcoated on a honeycomb substrate. The substrate used was mullite, three inches long with 1/16 inch square cells.

Experiments using a platinum washcoat and perovskite powder washcoats with nominal 0.1% (by weight) platinum (supplied by Transtech, Inc.) and with nominal 0.5%, 1.0% and 2.0% (by weight) platinum (supplied by Prof. Harlan Anderson, University of Missouri-Rolla) have been conducted. The tests consisted of establishing the light-off temperature and low temperature performance for several equivalence ratios and inlet velocities, after which the catalyst was "aged" for several hours at 1500°K and then the light-off and low temperature experiments repeated. The substrate temprature profile for a typcial aging run is shown in Figure 12. The purpose of running at low temperature is to insure that all of the heat release is due to surface reactions. Therefore the maximum substrate temperature in these runs was kept below 1050°K. Even at low temperatures however, it is important that the overall process be surface reaction rate controlled and not diffusion controlled. Then the measured substrate temperature profiles will provide an indication of changes in surface activity.

Figure 13 shows the substrate temperature profiles before and after aging
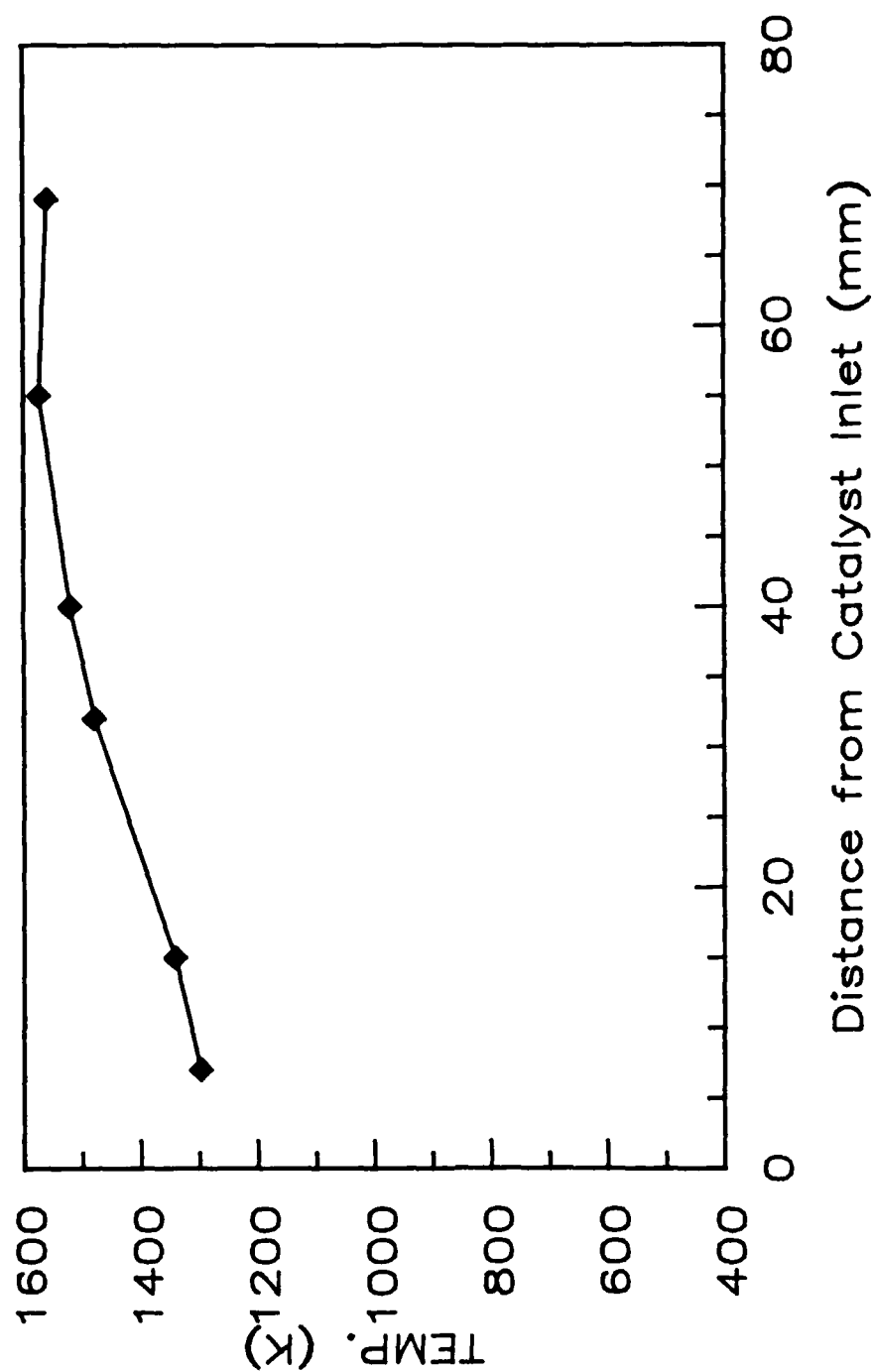
FIGURE 12.   AGING OF PURE PLATINUM CATALYST PROPANE FUEL, EQUIVALENCE
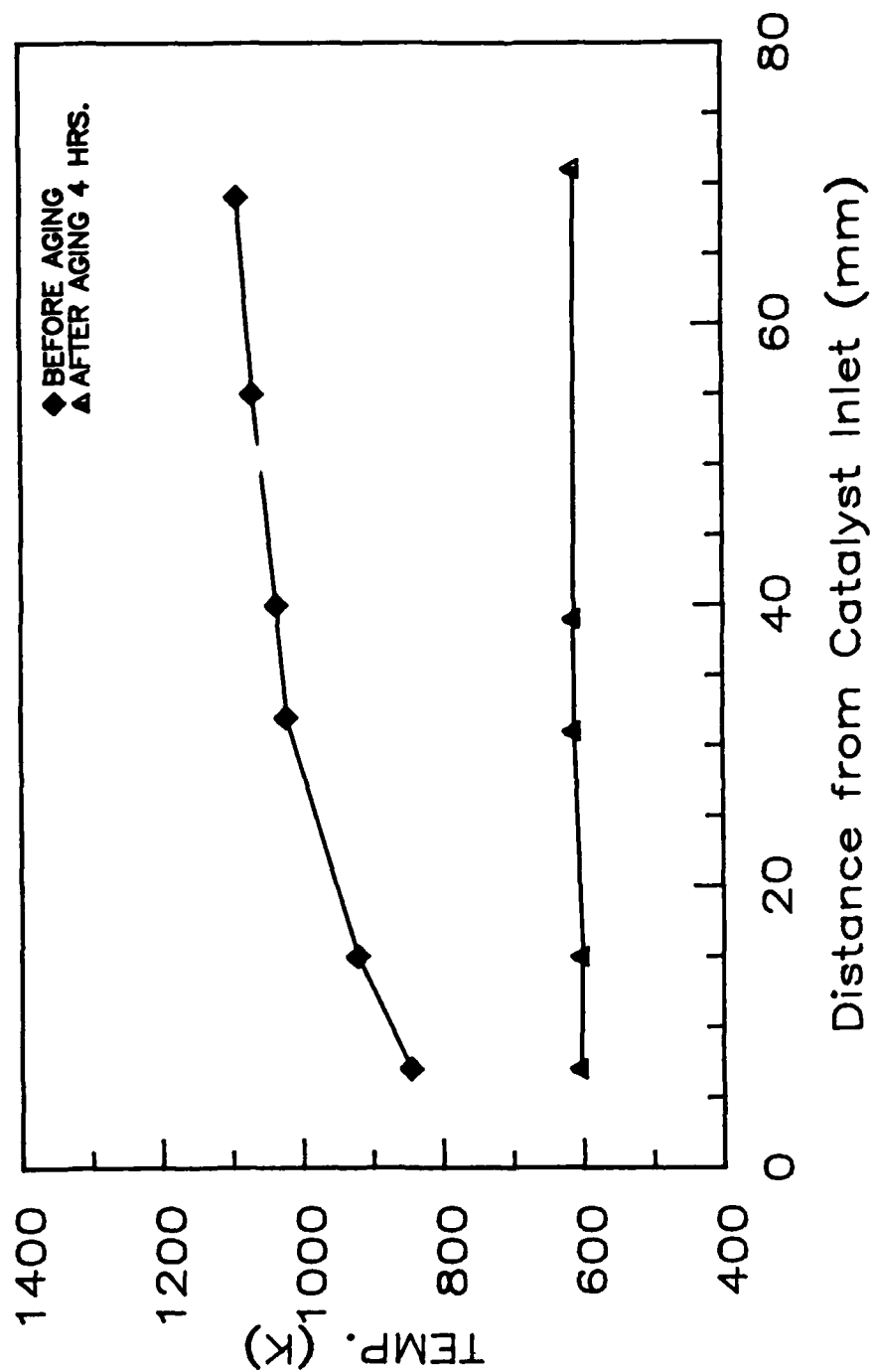RATIO = 0.42,   INLET TEMP. = 688K,   INLET VELOCITY = 9.9 m/s

FIGURE 13.   PURE PLATINUM CATALYST PROPANE FUEL, QUIVALENCE RATIO = 0.28
              INLET TEMP. = 589K, INLET VELOCITY = 10.1 m/s

for the platinum coated catalyst using propane fuel at an equilvalence ratio of
0.28, inlet temperature of 580°K, inlet velocity at 10 m/sec and 1 atmosphere
pressure. After aging for four hours at 1500°K the catalyst would not reignite
at these operating conditions, clearly indicating a loss of surface activity
which in this case is due to a loss of platinum as a result of vaporization.
The results for the same catalyst before and after aging using hydrogen fuel are
shown in Figure 14. In this case for the same catalyst there is no indication
of a change in surface activity. The reason for this is that hydrogen is so
reactive on platinum that the catalyst's performance is diffusion controlled
even after substantial platinum loss. These two cases are interesting in that
the first clearly demonstrates the problem of catalyst aging and the second
demonstrates the importance of evaluating the catalyst's surface activity under
surface reaction rate controlled conditions.

Figure 15 shows measured substrate temperature profiles for the perovskite
with nominal 1% by weight platinum using propane fuel at an equivalence ratio
of 0.3, inlet temperature of 700°K, inlet velocity of 6 m/sec, and 1 atmosphere
pressure. The before aging result is with the new catalyst. Also shown are
results after four successive aging runs. The indicated times are cumulative.
As the results show, there is a noticeable loss of activity after the second and
fourth aging runs which were done with a mixture of hydrogen and propane.
However, after the first and third aging runs, which were done with pure pro-
pane, there is little indication of reduced surface activity. These results are
very encouraging, indicating very little change in surface activity when used
with propane fuel. The tests with hydrogen however indicate a definite reduc-
tion in the activity of the catalyst.

In order to confirm these results plans were made to repeat the tests with
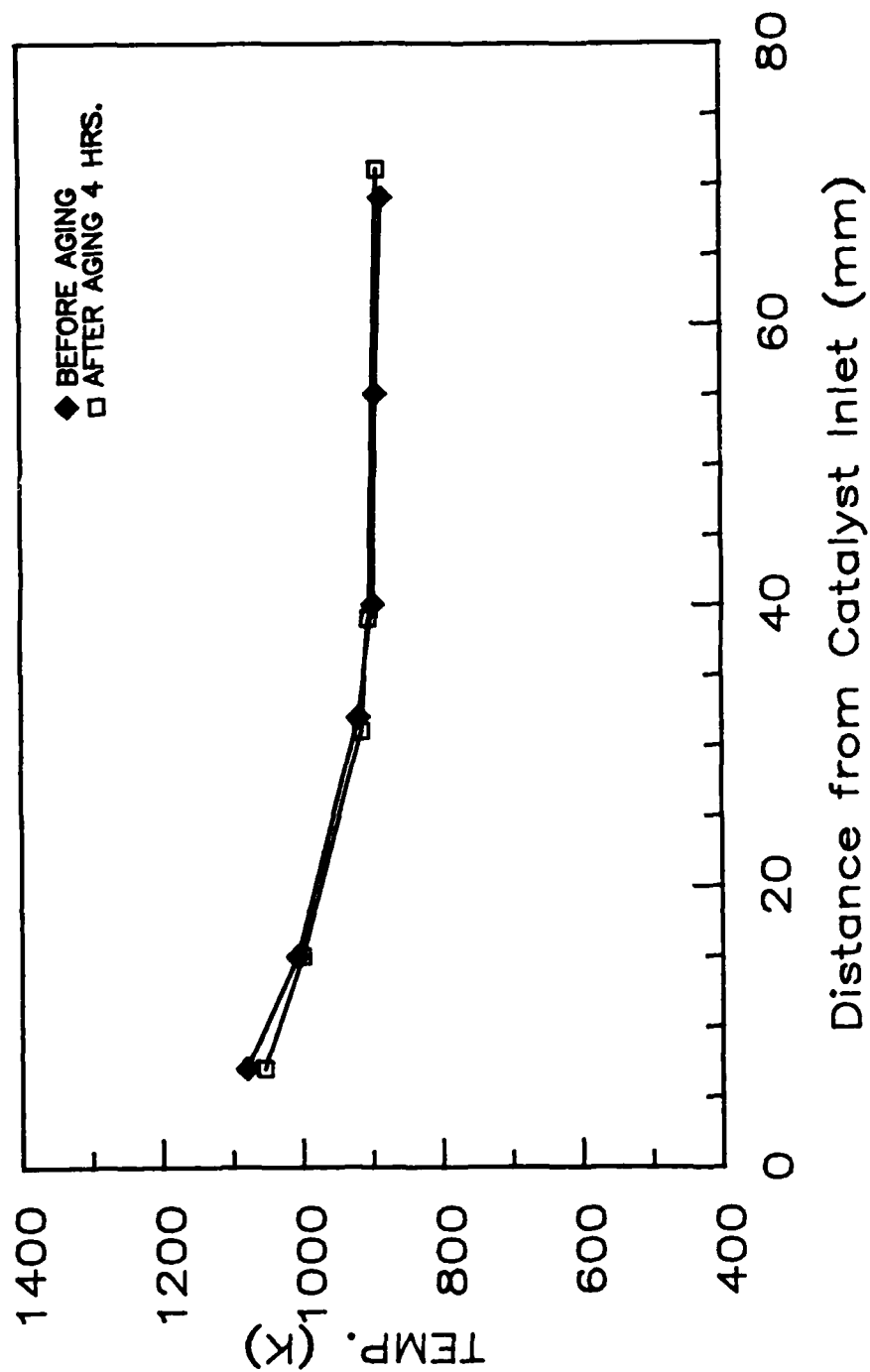the platinum doped perovskite using only propane during the aging runs. Three

FIGURE 14.   PURE PLATINUM CATALYST HYDROGEN FUEL, EQUIVALENCE RATIO = 0.1
INLET TEMP. = 590 K, INLET VELOCITY = 10.2 m/s
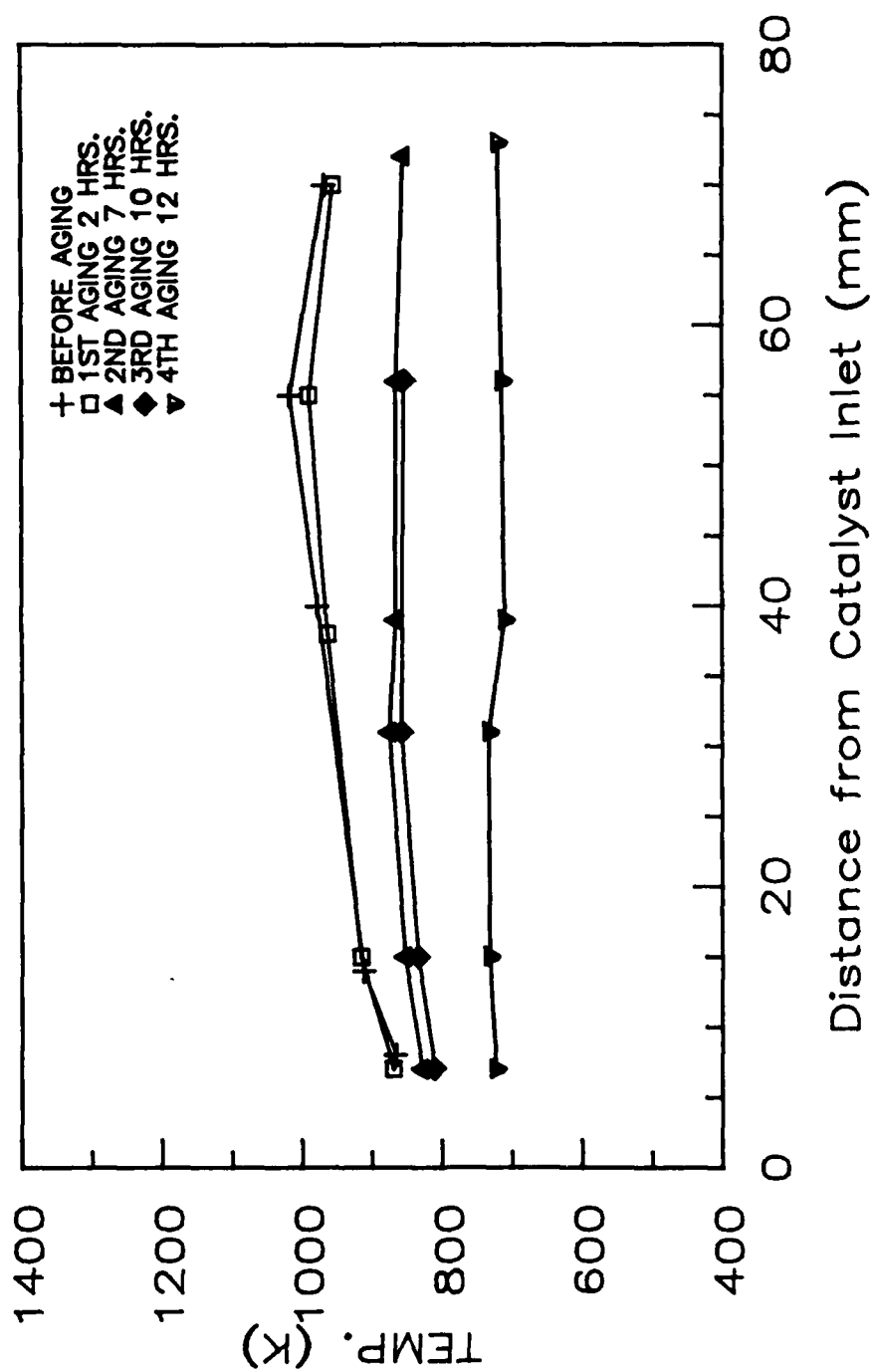
43

FIGURE 15.   PEROVSKITE WITH NOMINAL 1% BY WEIGHT PLATINUM CATALYST
              PROPANE FUEL, EQUIVALENCE RATIO = 0.30, INLET TEMP. = 698 K,
              INLET VELOCITY = 6.0 m/s

new catalysts were prepared with new perovskite powders (supplied by Prof. H. Anderson) having 0.5%, 1.0% and 2.0% by weight platinum content. A perovskite powder with 0.1% by weight platinum supplied previously by Transtech Inc. was also tested. The measured substrate temperture profiles with these four cata- lysts are shown in Figure 16 using propane fuel at an equivalence ratio of 0.3, inlet temperature of 800°K, inlet velocity of 10 m/sec, and 1 atmosphere pressure. Also shown for comparison is the corresponding temperature profile with the original 1% platinum catalyst. This comparison clearly shows that all four of the new catalyst samples were considerably less active than the original catalyst even though in one case the indicated platinum content was twice as great.

The remainder of this report is a summary of the status of the investiga- tion of the difference in surface activity between the new perovskite powders and the original, considerably more active 1% platinum doped perovskite powder. The first test was basically a confirmation of the flow reactor results. This involved testing the perovskite catalysts using a differential scanning calori- meter (DSC). This simply involves heating two small samples, one of the cata- lyst and the other an inert, in a temperature programmed oven and monitoring the temperature difference between the catalytic and the inert samples which is an indication of the heat release due to catalytic reactions. The oven can be filled with any fuel/air mixture to test the catalytic activity with respect to fuel identity and equivalence ratio. In addition to the original 1% sample and the new 0.1%, 0.5%, 1.0% and 2.0% samples, tests were run with platinum black and a perovskite powder with no platinum. The results from the DSC tests, run with propane in air at an equivalence ratio of 2.8, are shown in Figure 17 and basically confirm the flow reactor results. The temperature at which the heat release drastically increases can be thought of as a relative ignition tem-
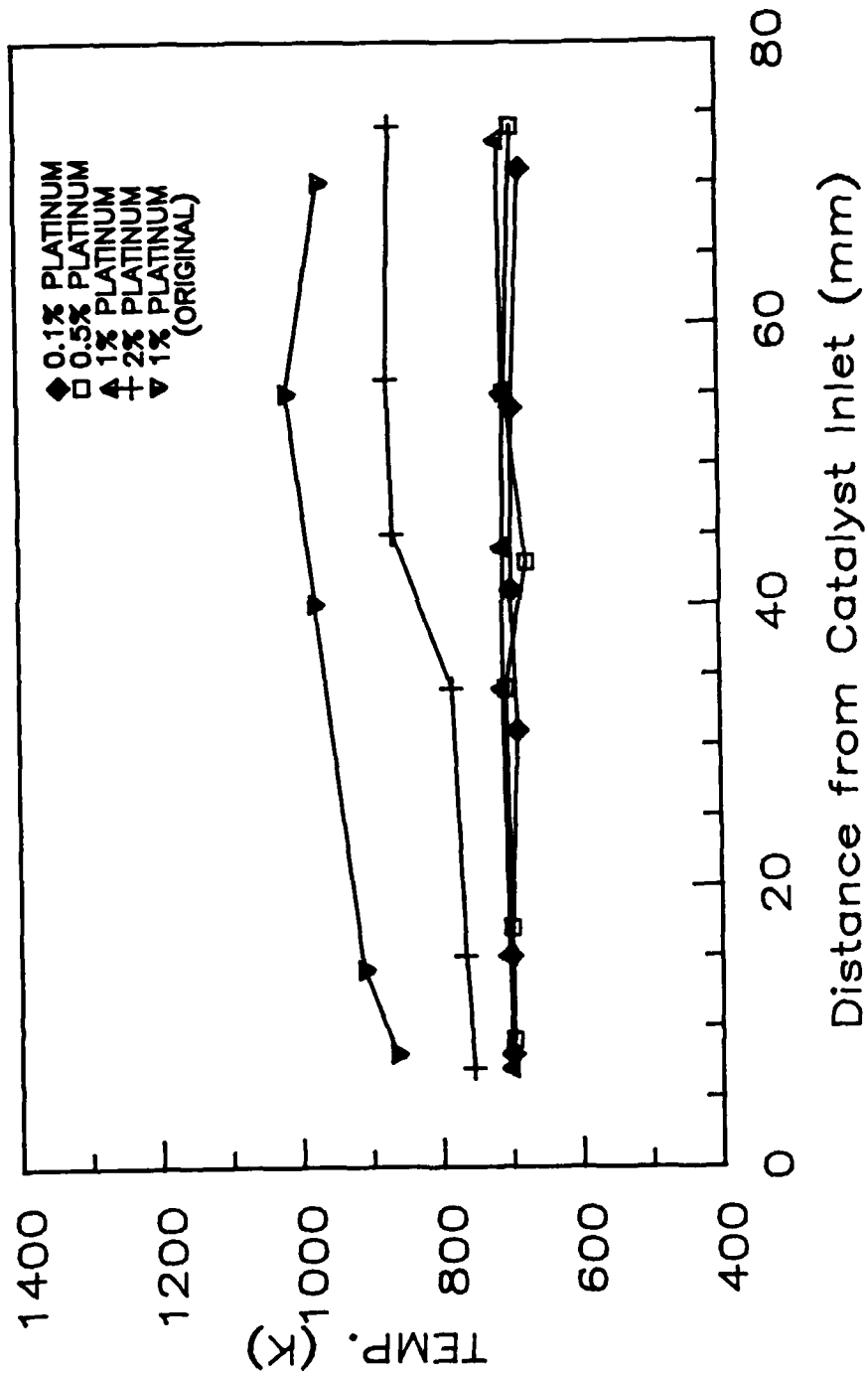
FIGURE 16.   PROPANE FUEL, EQUIVALENCE RATIO = 0.3, INLET TEMP. = 700K,
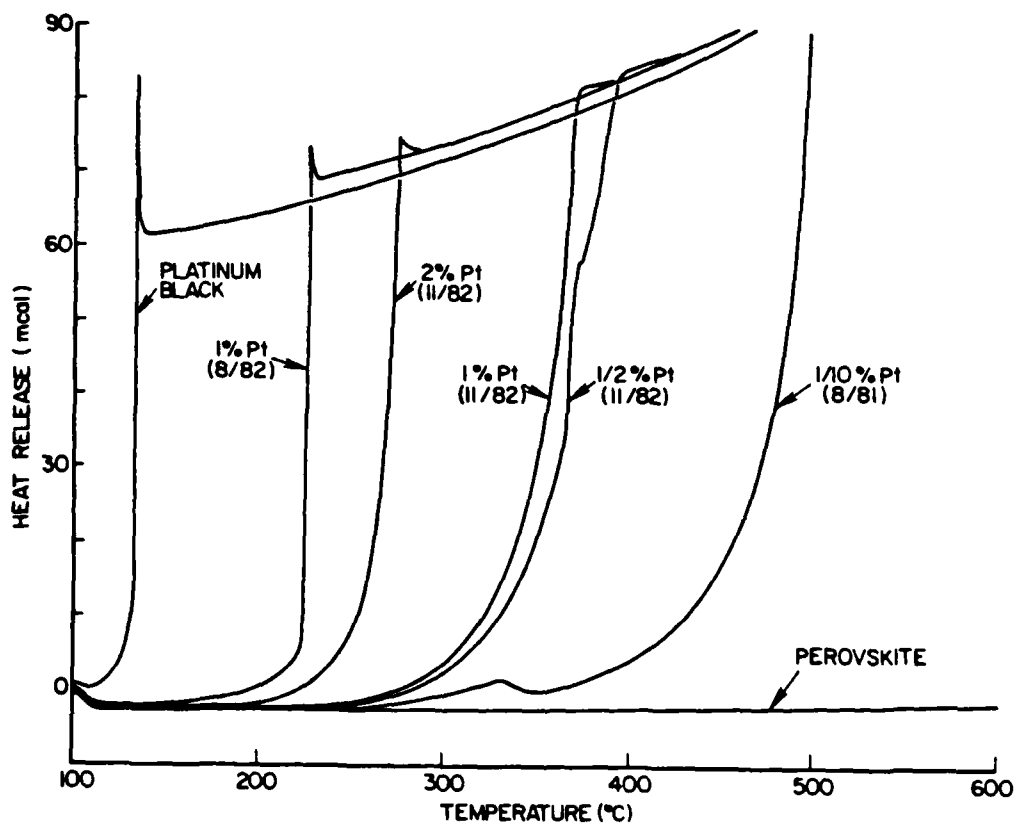   INLET VELOCITY = 10 m/s

FIGURE 17.   DIFFERENTIAL SCANNING CALORIMETRY TESTS OF RELATIVE CATALYTIC ACTIVITY
WITH PROPANE IN AIR AT AN EQUIVALENCE RATIO OF 2.8

perature. Note that the relative ignition temperatures of the new catalysts are consistent with their relative platinum content but that the original 1% sample is considerably more active, i.e. has a lower ignition temperature. In fact the original 1% catalyst is nearly as active as the platinum catalyst. An important outcome of the DSC testing was the demonstration that such a method could be used to determine the relative activity of catalyst samples with various fuel/air combinations. This has proven to be an efficient and convenient method of screening new catalysts before preparing a washcoated substrate and testing in the flow reactor.

After the differences in surface activity were confirmed with the DSC, several tests were made to establish the cause of this difference. The first of these tests involved using X-ray fluorescence to determine the actual platinum, chronium and lanthanum content of the perovskite catalyst samples. The results from these measurements are given in Tables 4, 5 and 6 where the absolute platinum composition and the relative chromium and lanthanum compositions are given. The measured platinum content was found to agree reasonably well with the expected platinum content. The small differences cannot explain the drastic differences in catalyst activity. The relative chromium and lanthanum compositions were found to be nearly the same in all samples and again the small differences cannot explain the differences in catalyst activity.

The second test involved scanning electron microscope studies of the crystal morphology and sintering. Photographs of the original 1% and the new 0.5%, 1.0% and 2.0% catalysts are shown in Figure 18 at a magnification of 5400. The basic conclusion from these photographs is that there is no difference in particle size, shape or degree of sintering that can explain the observed difference in catalytic activity.

The third test was BET measurements of the relative surface area. The

TABLE 4 - PLATINUM CONCENTRATION

SAMPLE	MEASURED CONCENTRATION
0.1% Pt (8/81)	0.1%
0.5% Pt (11/82)	0.34%
1.0% Pt (11/82)	1.03%
2.0% Pt (11/82)	2.32%
1.0% Pt (8/82)	0.98%

TABLE 5 - RELATIVE LANTHANUM CONCENTRATION

SAMPLE	MEASURED AREA
0.5% Pt (11/82)	9816
1.0% Pt (11/82)	9677
2.0% Pt (11/82)	9867
1.0% Pt (8/82)	9861

TABLE 6 - RELATIVE CHROMIUM CONCENTRATION

SAMPLE	MEASURED AREA
0.5% Pt (11/82)	45693
1.0% Pt (11/82)	48315
2.0% Pt (11/82)	49376
1.0% Pt (8/82)	45671

TABLE 7 - BET RELATIVE SURFACE AREA

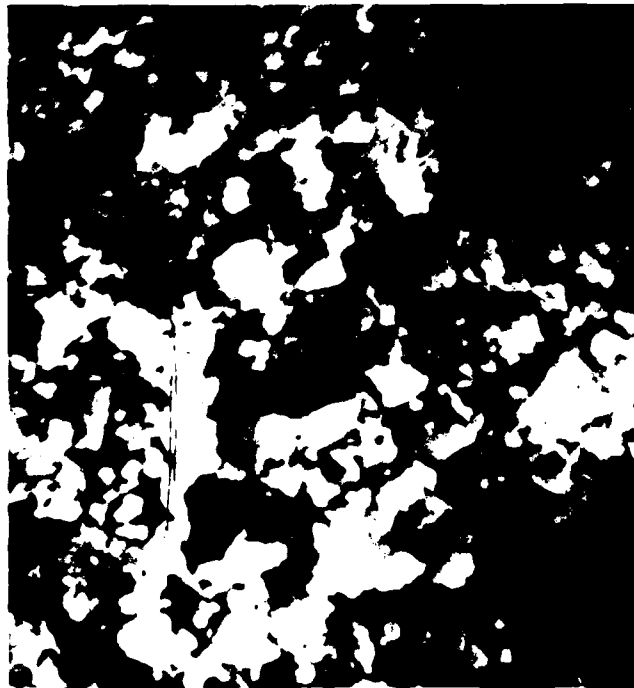| SAMPLE	SURFACE AREA
0.5% Pt (11/82)	8.073 m^2/g
1.0% Pt (11/82)	10.115 m^2/g
2.0% Pt (11/82)	6.876 m^2/g
1.0% Pt (8/82)	9.552 m^2/g
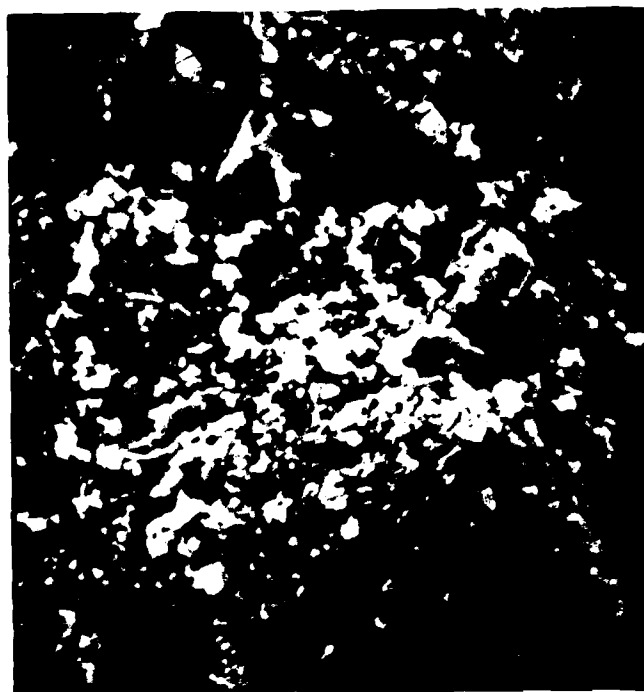
1.0% Pt (original)

2.0% Pt

Figure 18

1.0% Pt

0.5% Pt

Figure 18
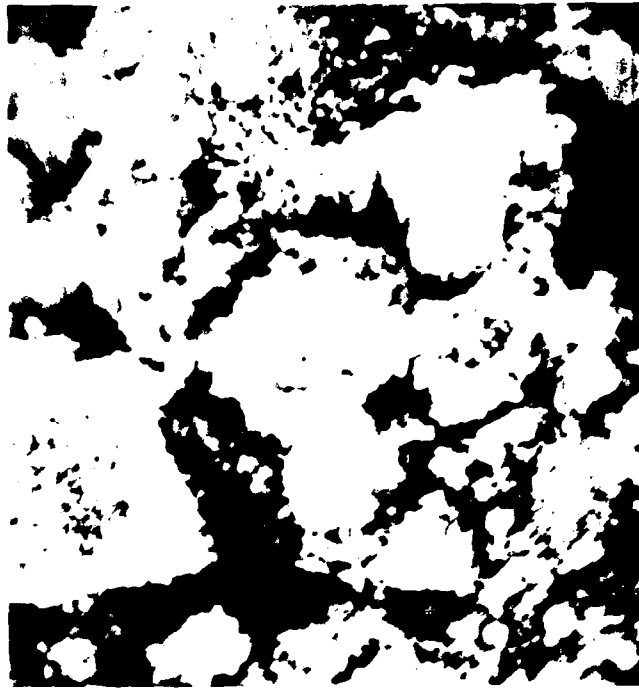
results of these tests are given in Table 7. Although there are differences in the effective surface area they do not correlate with the surface activity differences.

The fourth and final test to date involved the use of Fourier transform infrared spectroscopy (FTIR) to characterize the catalyst. FTIR spectra of the original 1% catalyst and the new 2% catalyst are shown in Figure 19. Although the spectral characteristics have not yet been identified there are definite differences in the two spectra, particularly near 3400 cm^{-1} and 1500 cm^{-1}, which may be related to the observed variations in catalytic activity. Work is continuing to identify the spectral characteristics which in turn may explain the observed differences in catalytic activity.

In summary, perovskite catalysts with small amounts of platinum have been shown capable of achieving low temperature light-off and high temperature stability in preliminary tests. Attempts to reproduce these results have revealed unexplainable variations in catalytic activity from sample to sample. Measurements of platinum, lanthanum and chromium composition, of crystal morphology and sintering, and or relative surface area have not provided an explanation for these differences in catalytic activity. Preliminary infrared spectra of the catalyst do show differences which may or may not be related to the observed variations in catalytic activity. Work is continuing to identify the spectral characteristics of the different perovskite samples, which in turn may provide insights to explain the differences in catalytic activity.

The idea of evaluating the relative performance of the catalysts in simple bench top experiments before actually testing them in the more complicated flow reactor experiments is very attractive. As mentioned earlier, the differential scanning calorimeter (DSC) has proven to be a simple and convenient method of characterizing the relative catalytic activity. In the final study covered in
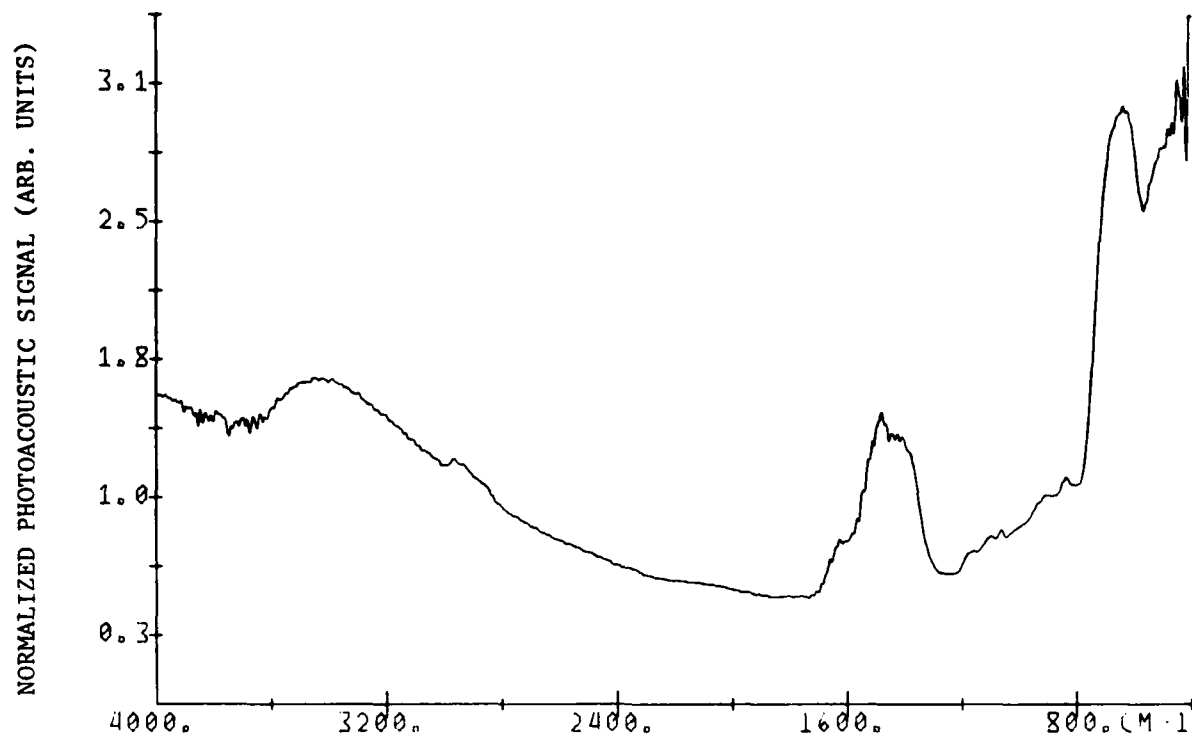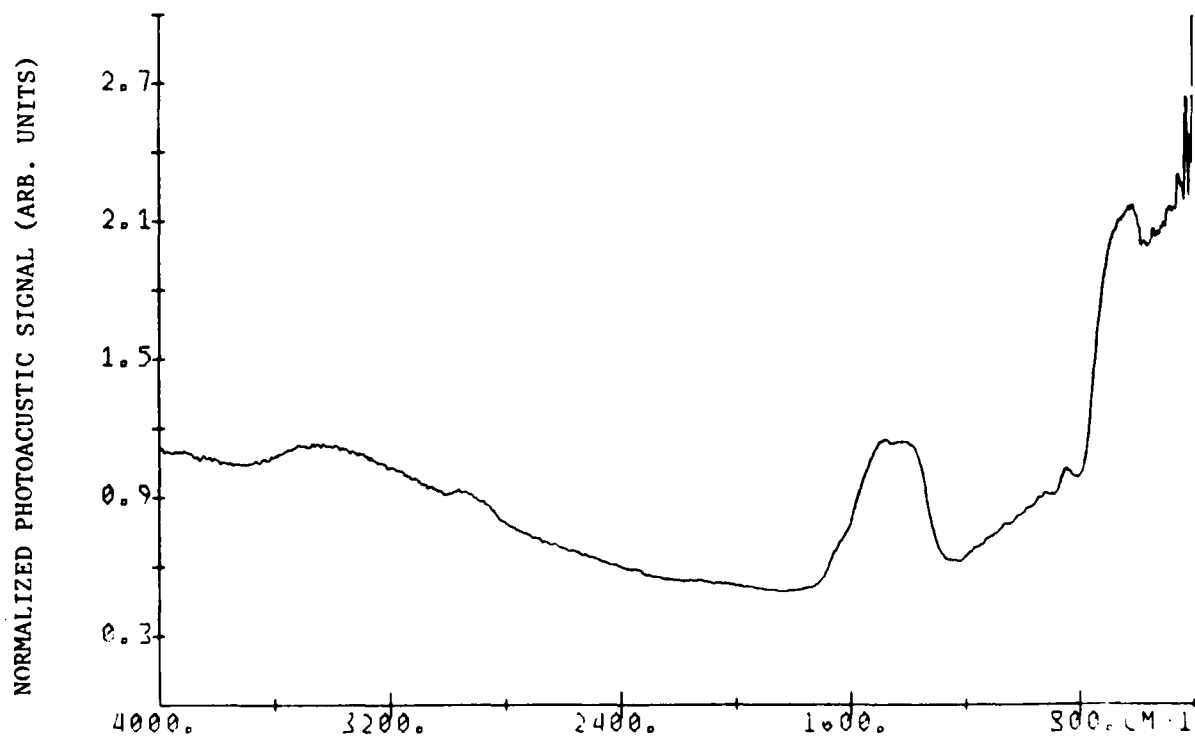
FIGURE 19a.   NEW 2% Pt IN PEROVSKITE

FIGURE 19b.   ORIGINAL 1% Pt IN PEROVSKITE

this report the DSC was used to characterize the "aging" of the 2% Pt-perovskite powder before and after exposure to high temperature in both oxygen and nitrogen environments. The samples were heated in a tube furnace to temperatures as high as 1500°K for periods of 4 hours. In Figure 20 the DSC plots for the new and various aged samples are given. As shown the catalytic activity drastically deteriorates in the high temperature oxygen environment whereas comparable aging in nitrogen shows no appreciable change in catalytic activity. Also shown is that the oxygen exposed catalysts can be substantially regenerated in a high temperature oxygen-free environment. At this point the effect of the oxygen on the catalyst is not understood.

Fourier transform infrared spectra of the new and variously aged 2% Pt-perovskite catalysts were also taken and are shown in Figure 21. There is however no apparent correlation between the infrared spectra and the observed catalyst aging phenomena.

At the conclusion of the grant period covered by this report work was continuing to determine the cause of these variations in catalytic activity.
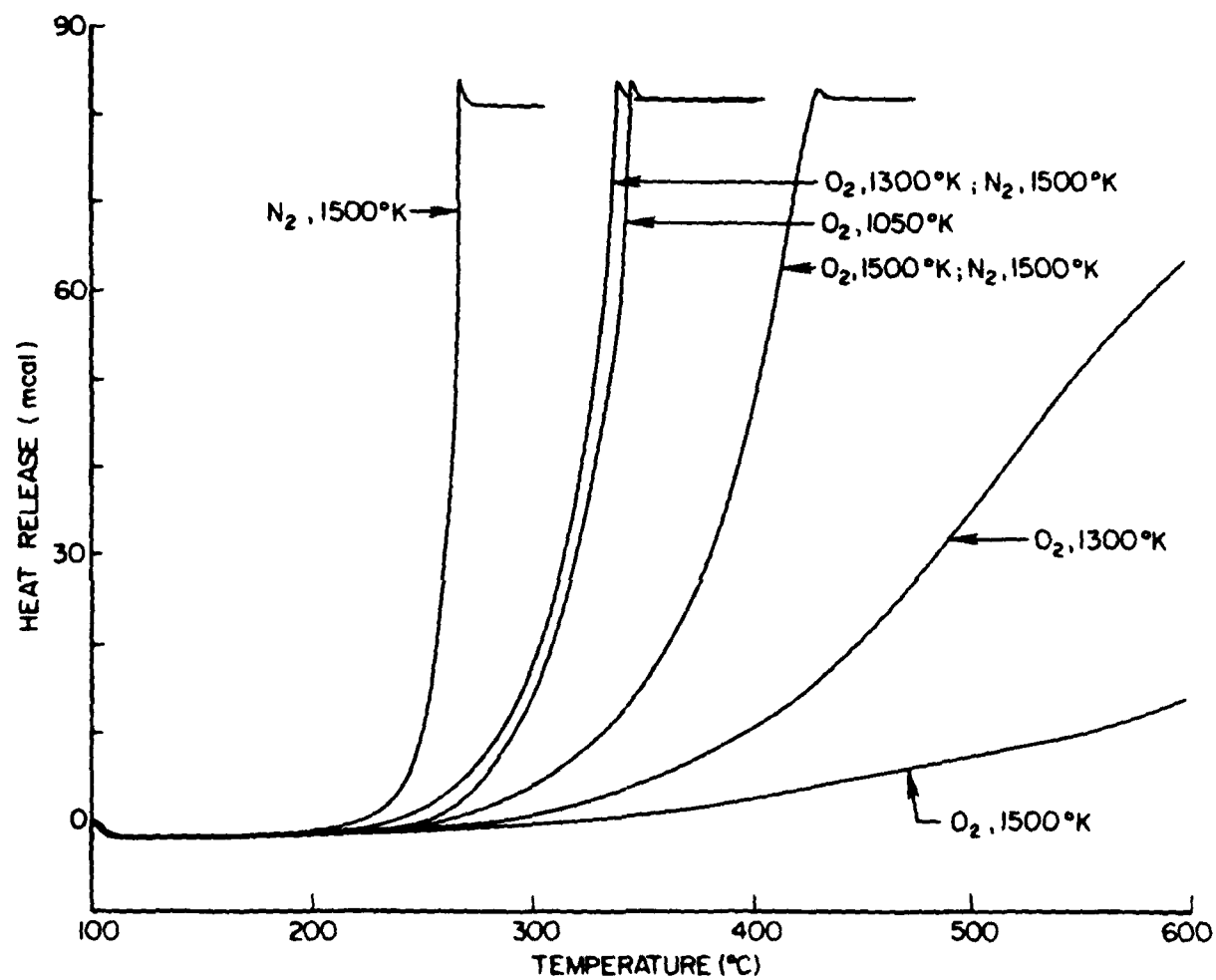
FIGURE 20. DIFFERENTIAL SCANNING CALORIMETER TESTS OF 2% Pt PEROVSKITE POWDER AFTER AGING
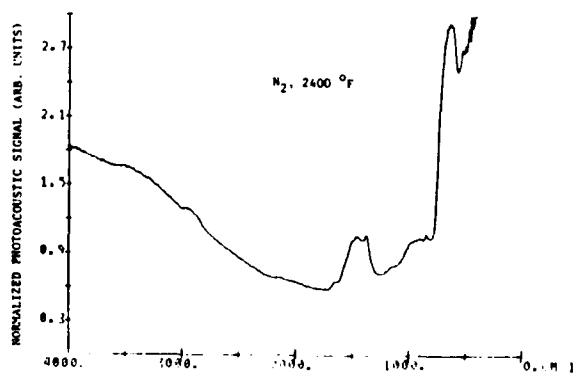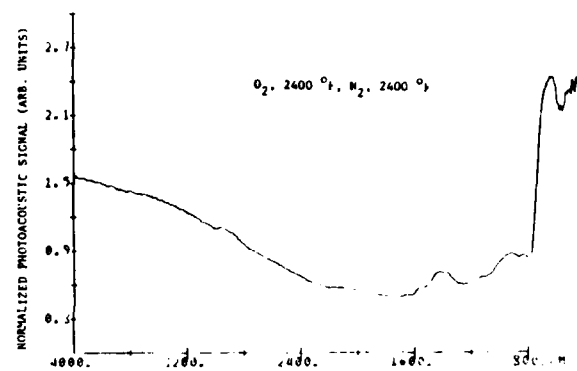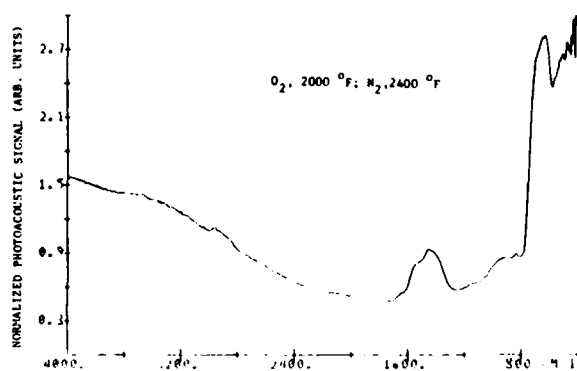
55

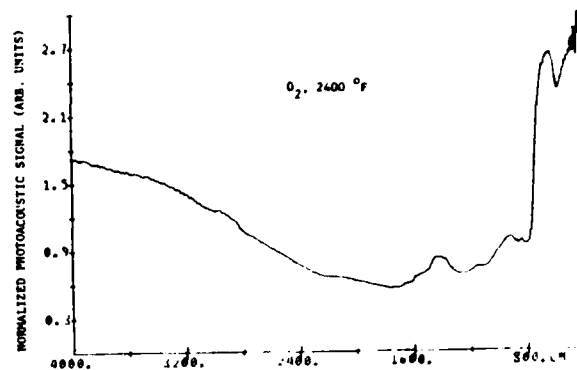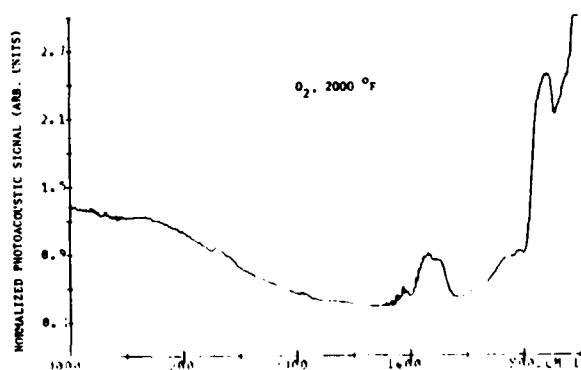FIGURE 21.   FOURIER TRANSFORM PHOTOACOUSTIC SPECTRA OF 2% Pt – PEROVSKITE
AFTER AGING

NOMENCLATURE

A	surface area of the catalyst, m^2
A_s	cross-sectional area of the substrate, m^2
C	radial heat loss constant
C_p	specific heat at constant pressure, J/kg-K
D_{ik}	binary diffusion coefficient, m^2/s
D	hydraulic diameter of the channel, m
E_o, E_s	activation energy for homogeneous and heterogeneous reactions, kcal/mole
h	enthalpy per unit mass, J/kg
k_o	pre-exponent for the homogeneous reaction rate, cm^3/mole-s
k_s	pre-exponent for the heterogeneous reaction rate, cm/s
K	thermal conductivity, J/m-s-K
ℓ	perimeter of the channel, m
L	length of the channel, m
$\dot{m}_{CO}$	CO mass consumption rate per unit area, kg/m^2-s
Nu	Nusselt number
p	pressure, N/m^2
q	heat flux, W/m^2
$\dot{q}_{catalytic}$	heat release rate due to heterogeneous reaction per unit area, W/m^2
Q	normalized heat transfer rate, or heat of combustion of homogeneous reaction, J/kg
r	channel radial coordinate, m
R	channel radius, m

57

$R°$ — universal gas constant cal/mole-K

s — thickness of the substrate, m

S_ϕ — source term

t — time, s

T — temperature, K

u — axial velocity, m/s

U_{in} — inlet velocity, m/s

v — radial velocity, m/s

V — volume of channel gas, m^3

W_k — molecular weight of species k

x — channel axial coordinate, m

X_k — mole fraction of species k

Y_k — mass fraction of species k

Greek Symbols

α — thermal diffusivity, m^2/s, or absorptivity

Γ — transport property

ϵ — emissivity

μ — gas viscosity, kg/m-s

ν — stoichiometric coefficient

ρ — density, kg/m^3

σ — cross-sectional area of the channel, m^2, or stress component, N/m^2, or Stefan Boltzmann constant, $W/m^2\text{-}K^4$

τ — non-dimensional time or characteristic time, s

ϕ — any dependent variable (such as u,v,p,...etc.), or equivalence ratio

$\dot{\omega}$ — reaction rate

Subscript

b	backward reaction
f	forward reaction, or face of the substrate, or final
g	gas
in, IN, 0	inlet, i.e. $x = 0$
k	species index
l	l-th homogeneous reaction
out, OUT, L	outlet, i.e. $x = L$
s	substrate
TS	test section
W	wall (substrate)

Superscript

'	reactant
"	product
+	substrate side of the interface
−	gas side of the interface

References

1. J.P. Kesserling, compiler, Proceedings: Fourth Workshop on Catalytic Combustion (Cincinnati, OH, May 1980), Environmental Protection Agency, Off. Res. Dev. Rep. 600/9-80-035, (1980).

2. S.M. DeCorso and D.C. Carl, "Structural Analysis of a Preliminary Catalytic Ceramic Design," Environ. Prot. Agency, Off. Res. Dev. Rep. 600/7-79-038, p. 139, (1979). Soc. Mech. Eng. Pap. 75-WA/Fu-1 (1975).

3. W.C. Pfefferle, R.V. Carrubba, R.M. Heck, and G.W. Roberts, "CATATHERMAL Combustion: a New Process for Low-Emissions Fuel Conversion," Am. Soc. Mech. Eng. Pap. 76-WA/Fu-1, (1975).

4. R.V. Carrubba, M. Chang, W.C. Pfefferle, and L.M. Polinski, "Catalytically Supported Combustion for Emission Control," Spec. Rep.-Electr. Power Res. Inst. (Palo Alto, CA) SR-39, p. 316 (1976).

5. S.M. DeCorso, S. Mumford, R. Carrubba, and R.M. Heck, "Catalysis for Gas Combustors," Am. Soc. Mech. Eng. Pap. 76-GT-4, (1976).

6. W.V. Krill and J.P. Kesselring, "The Development of Catalytic Combustors for Stationary Source Applications," Environ. Prot. Agency, Off. Res. Dev. Rep. 600/7-79-038, p. 259, (1979).

7. H. Fukuzawa and Y. Ishihara, "Catalytic Combustion for Gas Turbines," Environ. Prot. Agency, Off. Res. Dev. Rep. 600/9-80-035, p. 349, (1980).

8. W.S. Blazowski and G.E. Bresowar, "Preliminary Study of the Catalytic Combustor Concept as Applied to Aircraft Gas Turbines," Air Force Appl. Prop. Lab. Tech. Rep. TR-74-32, (1974).

9. T.J. Rosfjord, "Catalytic Combustion for Gas Turbine Engines," AIAA Paper 76-46, (1976).

10. V.J. Siminski and H.J. Shaw, "Development of a Hybrid Catalytic Combustor," J. Eng. Power, Vol. 100, p. 267, (1978).

11. A.J. Szaniszlo, "The Advanced Low-Emissions Catalytic Combustion Program Phase I - Description and Status," Environ. Prot. Agency, Off. Res. Dev. Rep. 600/7-79-038, p. 385, (1979).

12. L.C. Angello and R.J. Rosfjord, "Application of Catalytic Flame Stabilzation for Aircraft Afterburners," Environ. Prot. Agency, Off. Res. Dev. Rep. 600/7-79-038, p. 61, (1979).

13. I.T. Osgerby, R.M. Heck, R.V. Carrubba, C.C. Gleason, and E.J. Mularz, "Combustion Catalyst Study for Simulated Aircraft Idle Mode Operation," Environ. Prot. Agency, Off. Res. Dev. Rep. 600/9-80-035, p. 398, (1980).

14. D.N. Anderson, "Performance and Emissions of a Catalytic Reseator with Propane, Diesel and Jet A Fuels," NASA Tech. Mem. TM-73796, (1977).

15. D.N. Anderson, "Effect of Catalytic Reactor Length and Cell Density on Performance," presented at the U.S. Environ. Prot. Agency, Off. Res. Dev., Second Workshop on Catalytic Combustion, Raleigh, NC, June 21-22, 1977.

16. D.N. Anderson, "The Effect of Initial Temperature on the Performance of a Catalytic Reactor," NASA Tech. Mem. TM-78977, (1978).

17. D.N. Anderson, "Effect of Inlet Temperature on the Performance of a Catalytic Reactor," Environ. Prot. Agency, Off. Res. Dev. Rep. 600/7-79-038, p. 403, (1979).

18. D.N. Anderson, R.R. Tacina, and T.S. Mroz, "Catalytic Combustion for the Automotive Gas Turbine Engine," NASA Tech. Mem. TM X-73589, (1977).

19. A.E. Cerkanowicz, R.B. Cole, and J.G. Stevens, "Catalytic Combustion Modeling: Comparisons with Experimental Data," J. Eng. Power, Vol. 99, Series A, No. 4, p. 593, (1977).

20. J.P. Kesselring, W.V. Krill, and R.M. Kendall, "Design Criteria for Stationary Source Catalytic Combustors," West. Sect. Combust. Institute Paper 77-32, (1977).

21. J.S. T'ien, "Modeling of Transient Operation of Catalytic Combustion," Comb. Sci. and Tech., 26, p. 65, (1981).

22. C. Bruno, P.M. Walsh, D.A. Santavicca, N. Sinha, Y. Yaw, and F.V. Bracco, "Catalytic Combustion of Propane/Air Mixture on Platinum," Comb. Sci. and Tech. 31, p. 43 (1983).

23. Bruno, C. Walsh, P.M., Santavicca, D. and Bracco, F.V., "High Temperature Catalytic Combustion of $CO-O_2-N_2$, Ar, He, CO_2-H_2O Mixtures on Platinum," Int. J. Mass & Heat Transfer, 26, No. 8, p. 1109 (1983).

24. N. Sinha, "Two Dimensional Modeling of Catalytic Combustion," MSE Thesis, Princeton University, (1982).

25. Williams, F.A., Combustion Theory, Addison-Wesley Publishing Co., Reading, (1967).

26. A. Murty-Kanury, Introduction to Combustion Phenomena, Gordon and Breach Science Publ., N.Y., N.Y., 1977.

27. S. Gordon and B.J. McBride, "Computer Program For Calculation of Complex Chemical Equilibrium Compositions, Rocket Performance, Incident and Reflected Shocks and Chapman-Jouget Detonations," NASA SP-273, (1971).

28. I. Langmuir, "The Mechanism of the Catalytic Action of Platinum in the Reactions $2 CO + O_2 = 2 CO_2$ and $2 H_2 + O_2 = 2H_2O$," Trans. Faraday Soc., 17, p. 621, (1922).

29. L.N. Khitrin and L.A. Solovyeva, "Homogeneous-Heterogeneous Combustion of Carbon Monoxide in Narrow Tubes," in VII Symposium (International) on Combustion, Butterworths Scientific Publications, London, p. 532, 1959.

30. J.J. Carberry, Chemical and Catalytic Reaction Engineering, McGraw-Hill Book Co., NY, p. 460 (1976).

31. J.A. Strozier, Jr., G.J. Cosgrove, and D.A. Fischer, "Oxidation of CO on Pt and Pd," Surface Science, 82, p. 481 (1979).

62

32. R.C. Shishu, "Kinetics of Carbon Monoxide Oxidation Over Platinum Catalyst," Ph.D. Thesis, University of Detroit, p. 14, (1972).

33. V.I. Bykov and C.S. Yablonskii, "Steady-State Multiplicity in Heterogeneous Catalytic Reactions, Int. Chem. Engg., Vol. 21, No. 1, p. 142, (1981).

34. S.E. Voltz, C.R. Morgan, D. Liederman, and S.M. Jacob, "Kinetic Study of Carbon Monoxide and Propylene Oxidation on Platinum Catalysts," Ind. Eng. Chem. Prod. Res. Dev., Vol. 12, No. 4, p. 294 (1973).

35. C.T. Campbell, G. Entl, H. Kuipers, and J. Segner, "A Molecular Beam Study of the Catalytic Oxidation of CO on a Pt (111) Surface," J. Chem. Phys. 73 (11), p. 5862 (1980).   36.

J.B. Howard, G.C. Williams, and D.M. Fine, "Kinetics of Carbon Monoxide Oxidation in Postflame Gases," in XIV Symposium (International) on Combustion, The Combustion Institute, Pittsburgh, p. 975, (1973).

37. A.D. Gosman and F.J.K. Ideriah, "TEACH-T: A General Computer Program for Two-Dimensional, Turbulent, Recirculating Flow," Dept. Mechanical Engineering, Imperial College, London, (1976).

PUBLICATIONS

"Two Dimensional, Transient Catalytic Combustion of CO/Air on Platinum," N.
Sinha, C. Bruno, and F.V. Bracco, submitted to The International Journal of Heat
and Mass Transfer.

"Perovskite Catalysts for High Temperature Catalytic Combustion," D.A.
Santavicca, Y. Stein, and B.S.H. Royce, presented at Eastern States Section of
the Combustion Institute, Fall Meeting, December 1982.

PROFESSIONAL PERSONNEL

Professor F.V. Bracco

Professor B.S.H. Royce

Dr. C. Bruno

Dr. D.A. Santavicca

Ms. Y. Stein

Mr. N. Sinha

Degrees Awarded

Mr. N. Sinha - Masters Degree, August 1982

"Two Dimensional, Transient Modeling of Catalytic Combustion"

INTERACTIONS

During the period from 8/81 to 7/83 there were numerous visitors to the Princeton Catalytic Combustion Laboratory. Of particular importance were the visits of Dr. W. Pfefferle (private consultant), Dr. W. Retallick (private consultant), Dr. L. Hegedus (W.R. Grace), Dr. D. McKee (General Electric), Dr. D. Golden (SRI), and Dr. J. Latty (Dresser).

PATENT DISCLOSURES

No action has been taken by the University Patent .

END

FILMED

5-85

DTIC